iScience

CellPress

Article

Cysteine Dioxygenase Regulates the Epithelial Morphogenesis of Mammary Gland via Cysteine Sulfinic Acid

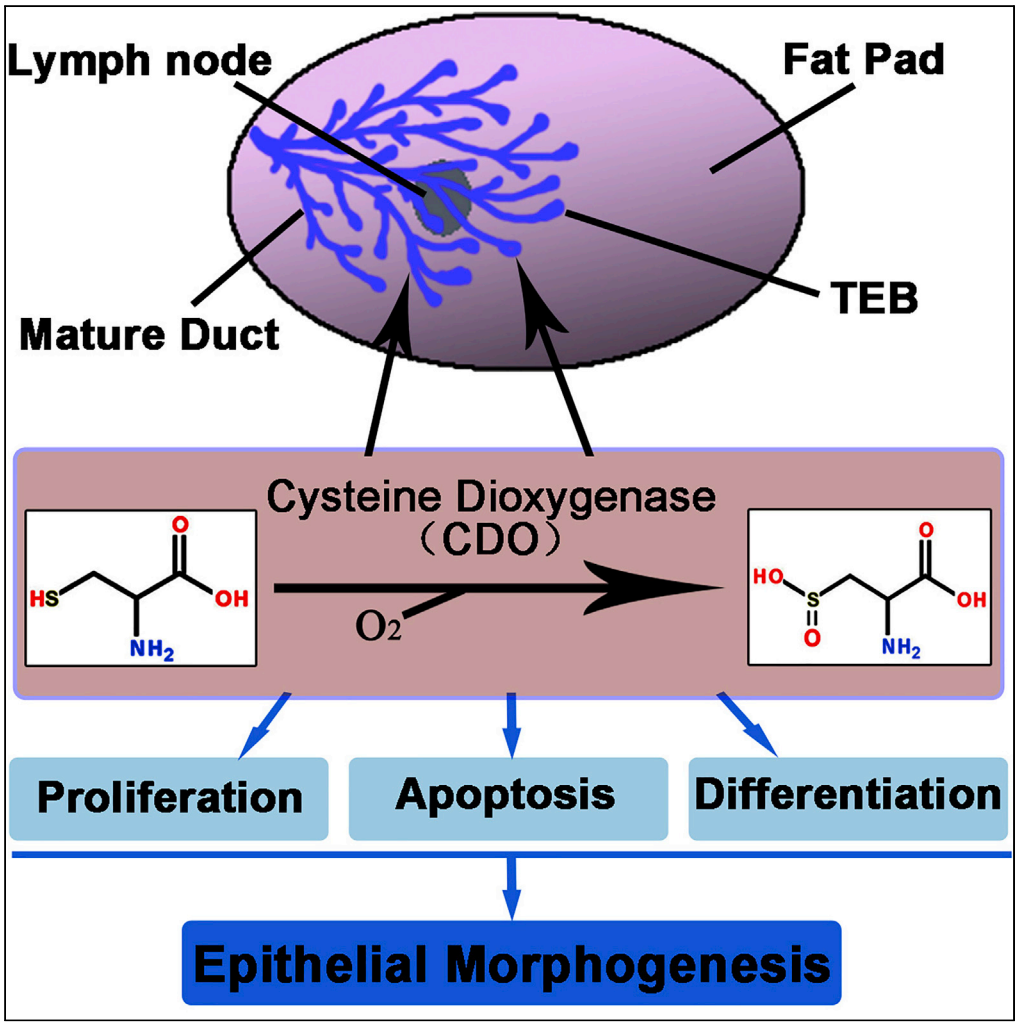

Jianjun Zhao, Yuzhu Han, Xingyu Ma, ..., Gongwei Zhang, Bingke Qiao, Anfang Liu

zhao8182@swu.edu.cn (J.Z.)
anfangliu@126.com (A.L.)

HIGHLIGHTS

Cysteine dioxygenase (CDO) is necessary for mammary epithelial morphogenesis

Cysteine sulfinic acid (CSA) supplementation rescues the mammary defects in CDO KO mouse

CDO retains lumen character and maintains luminal cell differentiation via CSA

CDO maintains epithelial cell renewal via CSA

Zhao et al., iScience *13*, 173–189
March 29, 2019
https://doi.org/10.1016/j.isci.2019.02.011

iScience

CellPress

Article

Cysteine Dioxygenase Regulates the Epithelial Morphogenesis of Mammary Gland via Cysteine Sulfinic Acid

Jianjun Zhao,[1,4,*] Yuzhu Han,[1] Xingyu Ma,[1] Yang Zhou,[1] Shukai Yuan,[2] Qian Shen,[3] Guogen Ye,[1] Hongrun Liu,[1] Penghui Fu,[1] Gongwei Zhang,[1] Bingke Qiao,[1] and Anfang Liu[1,*]

SUMMARY

Epithelial morphogenesis is a common feature in various organs and contributes to functional formation. However, the molecular mechanisms behind epithelial morphogenesis remain largely unknown. Mammary gland is an excellent model system to investigate the molecular mechanisms of epithelial morphogenesis. In this study, we found that cysteine dioxygenase (CDO), a key enzyme in cysteine oxidative metabolism, was involved in mammary epithelial morphogenesis. CDO knockout (KO) females exhibited severe defects in mammary branching morphogenesis and ductal elongation, resulting in poor lactation. CDO contributes to the luminal epithelial cell differentiation, proliferation, and apoptosis mainly through its downstream product cysteine sulfinic acid (CSA). Exogenous supplementation of CSA not only rescued the defects in CDO KO mouse but also enhanced ductal growth in wild-type mouse. It suggests that CDO regulates luminal epithelial differentiation and regeneration via CSA and consequently contributes to mammary development, which raises important implications for epithelial morphogenesis and pathogenesis of breast cancer.

INTRODUCTION

Epithelial morphogenesis contributes to organogenesis, functional formation, and regeneration, which play a fundamental role in animal development (Schock and Perrimon, 2002; Varner and Nelson, 2014). The mammary gland consists of a highly branched ductal epithelium surrounded by fatty stroma. Unlike other organs, mammary gland ductal epithelium morphogenesis is predominantly active after the onset of puberty (Watson and Khaled, 2008). The mammary epithelial morphogenesis involves the reiterative process of ductal branching and invasion into the surrounding mesenchyme, which is the base of organotypic growth of mammary parenchyma and important for functional formation (Macias and Hinck, 2012; Nelson et al., 2006; Watson and Khaled, 2008). Pubertal mammary gland is a good model that is utilized to study the molecular mechanisms of epithelial morphogenesis (Howlin et al., 2006; McBryan and Howlin, 2017; Medina, 1996).

The development and functional formation of mammary gland are vital for providing offspring nutrition and milk production. It undergoes several distinct stages including embryonic, neonatal, pubertal, pregnant, lactational, and involutional stages (Musumeci et al., 2015). Specialized structures named terminal end buds (TEBs) are formed at the end of growing ducts in pubertal mammary, which drives ductal branching morphogenesis and lumen formation by a highly regulated process of cell proliferation and death (Humphreys et al., 1996; Williams and Daniel, 1983). TEBs contain an outer layer of cap cells, which give rise to myoepithelial cells and multilayered body cells, which are the progenitors of luminal cells (Hennighausen and Robinson, 2005). Up to adult, the TEBs stop elongating and revert to simple epithelial architecture when they reach the edges of mammary fat pad and give rise to mature ductal tree (Nelson et al., 2006; Watson and Khaled, 2008). Mature ducts consist of two differentiated epithelial cell types, both deriving from a multipotent progenitor population. Myoepithelial cells present at the outer layer of the ducts form a sleeve around the primary ducts, and luminal epithelial cells situate in ductal lumen and secrete milk proteins (Huebner and Ewald, 2014; Shackleton et al., 2006; Van Keymeulen et al., 2011). The process of mammary epithelial morphogenesis and functional formation requires cell differentiation, proliferation, and apoptosis (Debnath et al., 2002; Kouros-Mehr et al., 2006; Mailleux et al., 2008). However, the underlying mechanisms of mammary epithelial morphogenesis remain unclear.

Cysteine dioxygenase (CDO) and cysteine sulfinic acid decarboxylase (CSAD), two key enzymes in cysteine oxidative metabolism and taurine biosynthesis, are present in the mammary gland (Ueki and Stipanuk,

[1]College of Animal Science, Southwest University, Chongqing, China

[2]College of Basic Medical Sciences, Tianjin Medical University, Tianjin, China

[3]Department of Microbiology, Ohio State University, Columbus, OH, United States

[4]Lead Contact

*Correspondence: zhao8182@swu.edu.cn (J.Z.), anfangliu@126.com (A.L.)

https://doi.org/10.1016/j.isci.2019.02.011

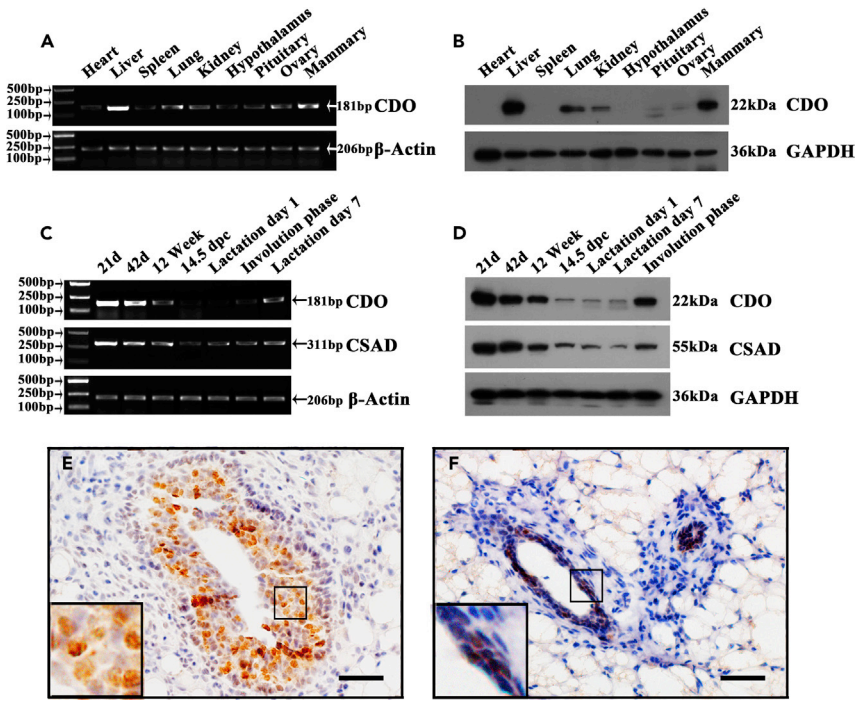

Figure 1. Expression of CDO in Mouse Mammary Gland

(A) CDO mRNA expression in various tissues of 6-week-old female mouse by RT-PCR.

(B) CDO protein production in various tissues of 6-week-old female mouse by western blot.

(C) The expression profile of CDO and CSAD mRNAs in mammary gland of different developmental stages.

(D) The production of CDO and CSAD proteins in mammary gland of different developmental stages.

(E) CDO localization in TEBs of pubertal mammary gland by immunohistochemistry (IHC) (brown stain).

(F) CDO localization in mature ducts of mammary gland by IHC (brown stain).

Scale bar = 50 μm.

2007). CDO is a mononuclear iron-dependent enzyme that catalyzes the oxidation of L-cysteine into cysteine sulfinic acid (CSA) (Driggers et al., 2013; McCoy et al., 2006; Simmons et al., 2006). CDO controls the intracellular content of cysteine and the diversity of sulfureted compounds in the body (Stipanuk et al., 2009; Ye et al., 2007). CSA can be decarboxylated by CSAD to form hypotaurine and is eventually oxidized into taurine (Peck and Awapara, 1967). The activity of CDO has important medical implications in Parkinson and Alzheimer diseases, systemic lupus erythematosus, and rheumatoid arthritis (Gordon et al., 1992; Heafield et al., 1990). In addition, CDO inactivation is associated with occurrences of various cancers (Brait et al., 2012; Jeschke et al., 2013; Meller et al., 2016). Whether the process of cysteine oxidative metabolism is involved in the mammary epithelial morphogenesis is still unknown. In this study, we found that CDO is highly enriched during mammary branching morphogenesis and localizes in body cells of TEBs and luminal epithelial cells in mature ducts. By mutation of CDO and CSAD we showed that CDO is necessary for mammary epithelial morphogenesis and maintenance of luminal epithelial differentiation and regeneration.

RESULTS

CDO Is Highly Enriched in the Mammary Gland during Ductal Branching Morphogenesis

We initially determined the expression profile of CDO in various tissues of 6-week-old female mouse by reverse-transcriptase polymerase chain reaction (PCR) (Table S1) and western blot (WB). The results showed that CDO transcription existed in all detected tissues; CDO expression was high in the liver, mammary gland, lung, and kidney, at both the mRNA and protein levels, but very low in the endocrine organs, including the hypothalamus, pituitary, and ovary of 6-week-old female mice (Figures 1A and 1B). During mammary gland development, CDO was abundant in the mammary gland of 21-day-old, 6-week-old, and 12-week-old virgin mice as well as in mice mammary gland of involution phase. In contrast, CDO

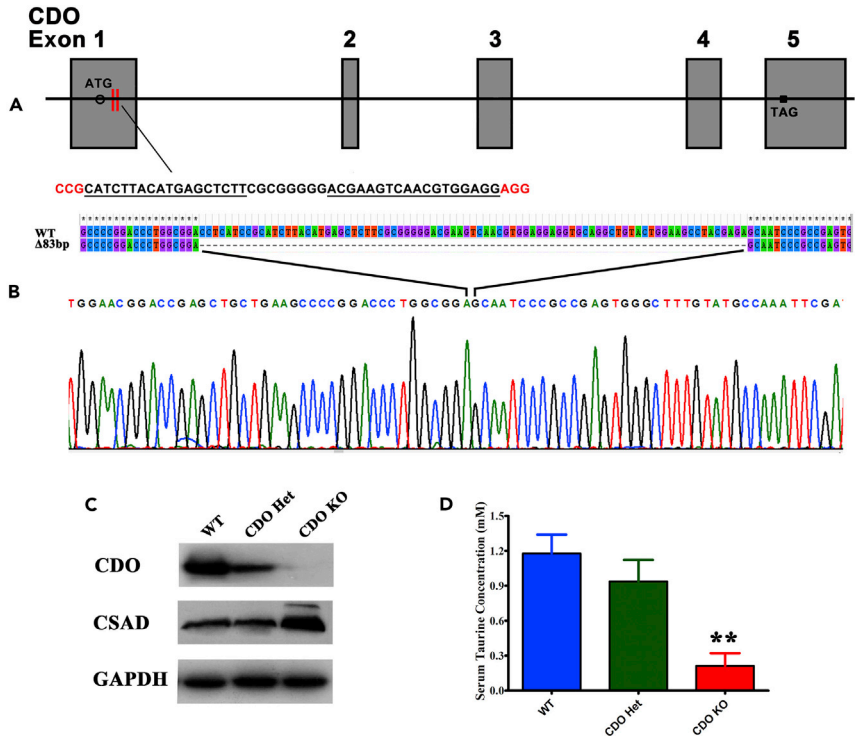

Figure 2. Generation and Confirmation of CDO KO Mice

(A) Murine CDO gene structure and Cas9n target information. The start codon of CDO (ATG) in the first exon is indicated in the black box. Two sgRNAs sequences are underlined, and PAM is indicated in red.

(B) After microinjection of the mixture of SpCas9n (D10A) mRNA (60 ng/μL) and sgRNAs (25 ng/μL) into cytoplasm of 0.5 dpc (days post-coitum) embryos, they were transferred to the oviduct of a pseudopregnant female. The F0 generation mice were genotyped by PCR and Sanger sequencing of targeted region. A mutation line of 83-nucleotide deletion (Δ83) in the codon region of CDO, which led to frameshift in protein sequence, was determined.

(C) CDO mutation was verified by western blot of wild-type (WT), CDO Δ83 heterozygote (CDO Het), and CDO Δ83 homozygote (CDO KO) mammary gland lysates (n = 2 mammary per genotype).

(D) Serum taurine levels of WT (n = 4), CDO Het (n = 4), and CDO KO (n = 4) mice assayed by high-performance liquid chromatography. CDO KO mice showed 82% reduction of serum taurine compared with WT (0.21 ± 0.11 versus 1.18 ± 0.16 mM) (t test, t-value = 7.855, p = 0.004).

was very low in the mammary gland of pregnant and lactating mice (Figures 1C and 1D). CSAD displayed similar expression profile to that of CDO (Figures 1C and 1D). These results indicated that CDO was enriched in mammary gland during ductal branching morphogenesis (e.g., puberty, non-pregnant, and non-lactating adult), but had low expression in alveolus stage (pregnant and lactating stage). We also determined the localization of CDO in mammary gland by immunohistochemistry. The results showed that CDO mainly localized to the luminal epithelial cells of mature duct (Figure 1F) and body cells of TEBs (Figure 1E) in 6-week-old mouse mammary. These data suggest that CDO in the mammary gland may be associated with mammary epithelial morphogenesis.

CDO Is Required for Mammary Development

To reveal the biological function of CDO and CSAD in mammary gland, we generated CDO knockout (KO) mice and CSAD KO mice via injection of SpCas9n (D10A) mRNA and a pair of single guide RNAs (sgRNAs) (Table S2) into mouse zygotes, as described in a previous study (Ran et al., 2013a, 2013b). Multiple mutant lines were confirmed by PCR and Sanger sequencing (Figures S1A and S1B, Table S3). A CDO KO mutant line with 83-nucleotide deletion in the first exon of mouse CDO and a CSAD KO mutant line with 32-nucleotide deletion in the second exon of mouse CSAD were used in the following experiments (Figures 2A, 2B, 3A, and 3B). Lack of CDO and CSAD proteins in KO mutant was verified by WB of mammary gland lysate (Figures 2C and 3C). Both CDO KO and CSAD KO mice exhibited systematic taurine deficiency (Figures 2D and 3D). We also observed that CDO KO mice had the phenotype of joint contracture at forelimb (Figure S1C), which was

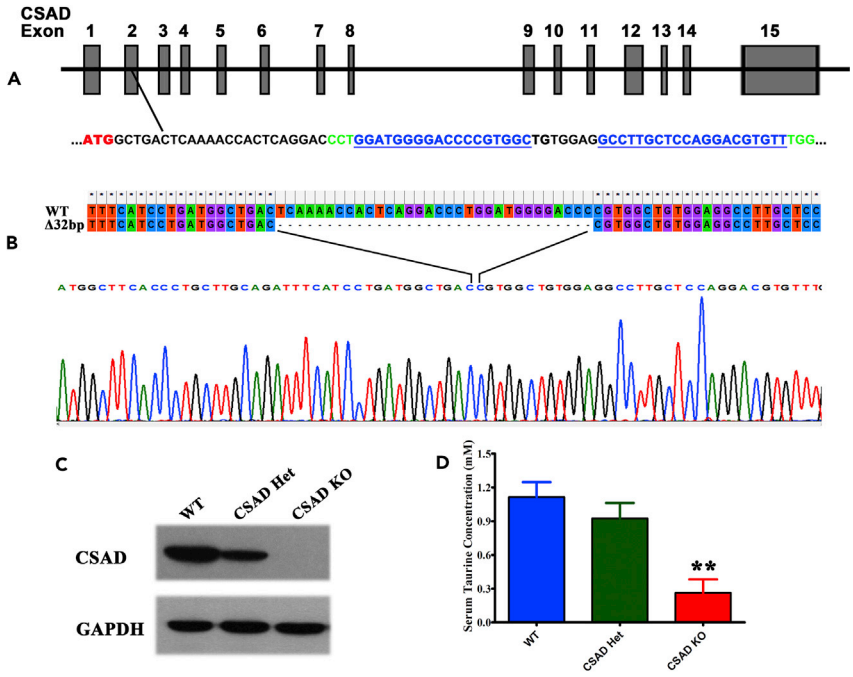

Figure 3. Generation and Confirmation of CSAD KO Mice

(A) Murine CSAD gene structure and Cas9n target information. ATG in red is the start codon of CSAD in the second exon followed by two truncated Cas9n targets (sgRNAs' spacer in blue and PAM in green).

(B) After microinjection of SpCas9n (D10A) mRNA (60 ng/μL) and sgRNAs (25 ng/μL) into cytoplasm of 0.5 dpc (days post-coitum) embryos, they were transferred to the oviduct of a pseudopregnant female. The F0 generation mice were genotyped by PCR and Sanger sequencing of target region. A mutation line of 32-nucleotide deletion (Δ32) in codon region of CSAD, which leads to frameshift in protein sequence, was determined.

(C) CSAD mutation verified by western blot of WT, CSAD Δ32 heterozygote (CSAD Het), and CSAD Δ32 homozygote (CSAD KO) mammary gland protein (n = 2 mammary per genotype).

(D) Serum taurine level of WT (n = 4), CSAD Het (n = 4), and CSAD KO (n = 4) mice were determined by high-performance liquid chromatography. CSAD KO mice showed 78% reduction of serum taurine compared with WT (0.26 ± 0.12 versus 1.12 ± 0.13 mM) (t test, t-value = 9.025, p = 0.003) **p<0.01.

consistent with a previous report (Ueki et al., 2011). In addition, CDO KO mice tend to have more large alveoli, which may result in decreased total alveoli number and alveolar surface area (Figure S1D).

We subsequently carried out whole-mount analysis of the fourth mammary gland from wild-type (WT), CSAD KO, and CDO KO virgin female mice in different developmental stages. Compared with WT mammary, CSAD KO mammary developed normally and had no significant difference in ductal elongation and branching (Figures 4A and 4B). In contrast, CDO KO mammary showed severe impairment in mammary development of ductal branching morphogenesis and elongation (Figure 4C). The mammary ductal elongation of TEBs exceeded the lymph node and generated a lot of branches in 42-day-old WT and CSAD KO mice, but in CDO KO mammary the duct TEBs could not reach the lymph node and branches were rather few. At the age of 12 weeks, the duct invaded into the fat pad and was bestrewed in WT and CSAD KO mice, whereas in CDO KO mammary, the duct just reached the lymph node and the branches were far from filling the fat pad. The ducts were not capable of filling the mammary fatty stroma by 24 weeks postpartum in CDO KO mice (Figure 4C). CDO heterozygous (CDO Het) mammary showed no obvious defect in ductal morphogenesis within the age of 12 weeks (Figure 4D). Quantitative analysis was carried out on the length of ductal invasion and the number of branches and TEBs. It showed that the duct invasion in the stroma of CDO KO mammary was much slower than that of WT and CSAD KO mice at age 42 days and 12 weeks (Figure 4E). Both the number of branches and TEBs were extremely low in CDO KO females compared with WT and CSAD KO mice (Figures 4F and 4G). We determined pituitary growth hormone (GH) and prolactin (PRL) by WB; the results indicated that CDO did not influence the synthesis of GH and PRL (Figure S2). CDO KO females were fertile, got pregnant properly, and gave birth at term with normal litter size (Table S4). To rule

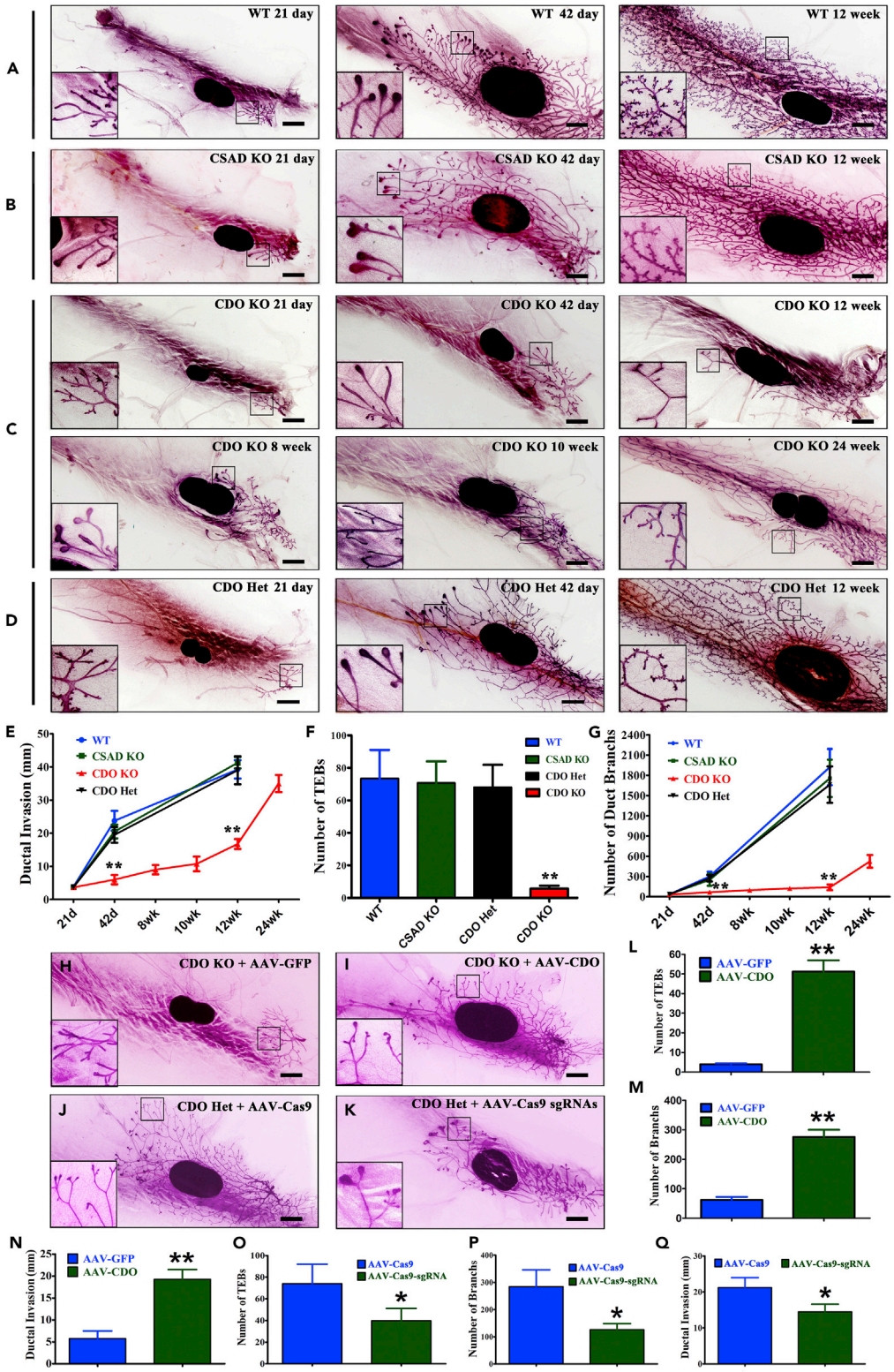

Figure 4. Loss of CDO Causes Mammary Developmental Defect in Ductal Invasion and Branching

(A–D) Carmine-stained fourth mammary gland whole-mount of (A) WT (n = 4 mammary per time point), (B) CSAD KO (n = 4 mammary per time point), (C) CDO KO (n = 5 mammary per time point), and (D) CDO Het (n = 4 mammary per time point) mice at different age of ducts morphogenesis.

Figure 4. *Continued*

(E) Length of ductal invasion (represented as distance from initial point of primary duct to distal TEBs or far end of the primary duct) in WT, CSAD KO, and CDO KO mammary glands at different ages (WT versus CDO KO, t test: 42 days, t-value = 11.889, p = 0.001; 12 weeks, t-value = 13.175, p = 0.001).

(F) Number of TEBs in 42-day-old WT, CSAD KO, and CDO KO mammary glands (WT versus CDO KO, t test: t-value = 7.419, p = 0.005).

(G) Number of branches in WT, CSAD KO, and CDO KO mammary glands at different ages (WT versus CDO KO, t test: 42 days, t-value = 7.527, p = 0.005; 12 weeks, t-value = 7.924, p = 0.004).

(H and I) Carmine-stained fourth mammary gland whole-mount duct morphogenesis of 42-day-old CDO KO mice with injection of control AAV (AAV-GFP) into one side of fourth mammary (H) and CDO expression AAV (AAV-CDO) into another side (I) at the age of P10 (n = 4).

(J and K) Carmine-stained fourth mammary gland whole-mount duct morphogenesis of 42-day-old CDO Het mice with injection of SaCas9 control AAV (AAV-Cas9) into one side of fourth mammary (J), and SaCas9-sgRNA AAV (AAV-Cas9-sgRNAs) into another side (K) at the age of P10 (n = 4).

(L) Number of TEBs in the mammary gland injection with CDO expression AAV (AAV-GFP versus AAV-CDO t test: t-value = −7.905, p = 0.004).

(M) Number of branches in the mammary gland injection with CDO expression AAV (AAV-GFP versus AAV-CDO t test: t-value = 6.563, p = 0.007).

(N) Length of ductal invasion in the mammary gland injection with CDO expression AAV (AAV-GFP versus AAV-CDO t test: t-value = −10.205, p = 0.002).

(O) Number of TEBs in the mammary gland injection with Cas9-sgRNA AAV (AAV-Cas9 versus AAV-Cas9-sgRNA t test: t-value = 3.759, p = 0.033).

(P) Number of branches in the mammary gland injection with Cas9-sgRNA AAV (AAV-Cas9 versus AAV-Cas9-sgRNA t test: t-value = 4.516, p = 0.02).

(Q) Length of ductal invasion in the mammary gland injection with Cas9-sgRNA AAV (AAV-Cas9 versus AAV-Cas9-sgRNA t test: t-value = 3.576, p = 0.037). Scale bar, 2 mm. * represents significant difference with control ($p < 0.05$), ** represents significant difference with WT or control ($p < 0.01$).

out the effect of lack of CDO in other organs, we carried out adeno-associated virus (AAV)-mediated mammary-gland-specific expression and KO CDO by *in situ* injection of AAV into the fourth mammary gland. AAV serotype 2 was used in this study. Mouse CDO expression and control AAV vector were constructed for packaging AAV (Figure S3A). The CDO KO mice were injected with CDO expression AAV or control AAV subcutaneously at the site of the fourth mammary nipple at the age of P10 for CDO rescue in mammary gland. The validity of the CDO expression and control AAV was determined by detecting green fluorescence and CDO expression assay in the mammary gland 2 weeks after injection. It showed strong green fluorescence and rescued CDO expression in the mammary (Figures S3B and S3C). Whole-mount analysis of the mammary indicated that rescue of CDO expression in mammary significantly improved ductal elongation, branching, and TEB number at P42 (Figures 4H, 4I, 4L–4N). The previously described AAV vector pX601 (Ran et al., 2015) was used to package CDO KO (constructed with an sgRNA spacer) or control (without sgRNA) AAV (Figure S3D). For high efficiency of SaCas9-mediated CDO KO in mammary gland, the AAVs with two highly specific SaCas9 targets of mouse CDO were mixed for injection (Table S5). The CDO Het females were injected with a CDO KO AAV (SaCas9 with sgRNA) or control AAV (SaCas9 without sgRNA) subcutaneously at the site of the fourth mammary nipple at the age of P10. The CDO expression in the mammary gland was determined after 2 weeks of first injection. It showed significant decrease of CDO expression in the mammary (Figure S3E). Whole-mount analysis of the mammary indicated that KO of CDO by AAV-Cas9-sgRNA injection in the mammary significantly influenced ductal morphogenesis (Figures 4J, 4K, and 4O–4Q), which confirmed the function of CDO in mammary development. These data suggest that CDO in mammary gland is involved in ductal branching morphogenesis.

We examined the microstructure of mammary gland in CDO KO, CSAD KO, and WT mice by hematoxylin and eosin (H&E) stain. The results showed that the tissue structure was mainly normal in 42-day-old CDO KO and CSAD KO mammary of mature ducts and TEBs with well-organized epithelial cells in the ducts (Figures 5A–5F), but that a disorganized and detached multilayered luminal epithelium developed in ducts in 12-week-old CDO KO mammary and also that there was disruption of the ductal architecture (Figures 5G–5I). In addition, we observed that CDO mutant females had a higher risk of breast tumors at the age of 12 weeks. We occasionally observed that CDO KO and CDO heterozygote mice got breast tumor, but no case was found in other genotypes (Figure S4). These results suggest that CDO is required to maintain lumen and cell viability of epithelium in mammary.

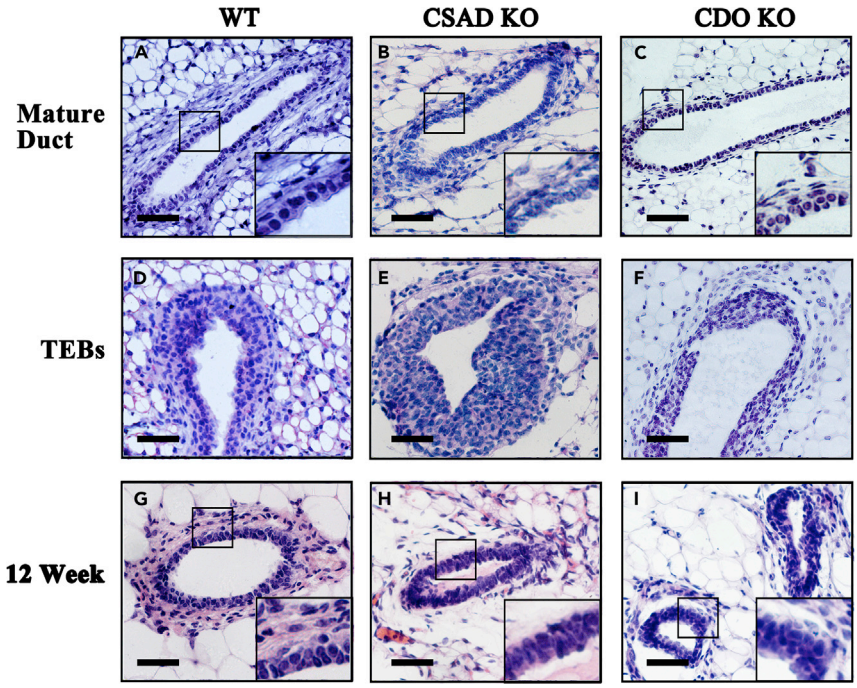

Figure 5. Microstructure Analysis of CDO KO Mammary Gland

Hematoxylin and eosin (H&E) staining of paraffin-embedded sections of murine mammary gland.

(A–C) Microstructure of mature ducts in 42-day-old (A) WT, (B) CSAD KO, and (C) CDO KO mice mammary glands (n = 4 mammary per treatment).

(D–F) Microstructure of TEBs in 42-day-old (D) WT, (E) CSAD KO, and (F) CDO KO mice mammary glands (n = 4 mammary per treatment).

(G–I) Microstructure of mature ducts in 12-week-old (G) WT, (H) CSAD KO, and (I) CDO KO mice mammary glands (n = 4 mammary per treatment). Scale bar, 50 μm.

Loss of CDO Leads to Lactation Insufficiency

We found that both CDO KO and CSAD KO mice can get pregnant mating with a WT male and give birth at term. However, the offspring of CDO KO mother grew retardedly and tended to die before weaning, in contrast to the offspring of CSAD KO mother, which grew well in the pre-weaning period. Whole-mount and microstructure analysis of the mammary gland in lactation period revealed that the mammary gland of CSAD KO mothers developed normally, even with more intensive mammary gland alveolus compared with WT (Figures 6C and 6D). However, CDO KO mothers exhibited severe defects in lactation such as reduction in the number and size of milk-producing alveolar units (Figures 6E and 6F) compared with WT mothers (Figures 6A and 6B). Owing to the lactation defect, the offspring of CDO KO mothers displayed a significant reduction in weight during suckling period, and they were apt to die at day 15 post-partum. When nursing them with a WT foster mother, the offspring of CDO KO mothers grew normally, and almost all of them survived to weaning (Figures 6G and 6H). These data suggest that loss of CDO results in poor lactation performance, which could be the consequence of developmental defects in mammary duct branching morphogenesis.

CSA Supplementation Rescues the Ductal Branching Morphogenesis of CDO KO Mice and Promotes Mammary Development of WT Mice

As a major catabolic enzyme of cysteine catabolism, CDO catalyzes by adding dioxygen to cysteine to form CSA (Joseph and Maroney, 2007; McCoy et al., 2006; Simmons et al., 2006). CSA is decarboxylated by CSAD to form hypotaurine, which is subsequently oxidized into taurine spontaneously in cells (Stipanuk et al., 2006) (Figure 7A). We measured CSA levels in the serum and mammary gland of WT, CDO KO, and CSAD KO mice using high-performance liquid chromatography. The result showed that CSA was almost not detected in any tissue of CDO KO mice, but that it increased in CSAD KO mice, both in serum and mammary tissue compared with WT (Figures 7B and 7C). According to cysteine-metabolizing pathway,

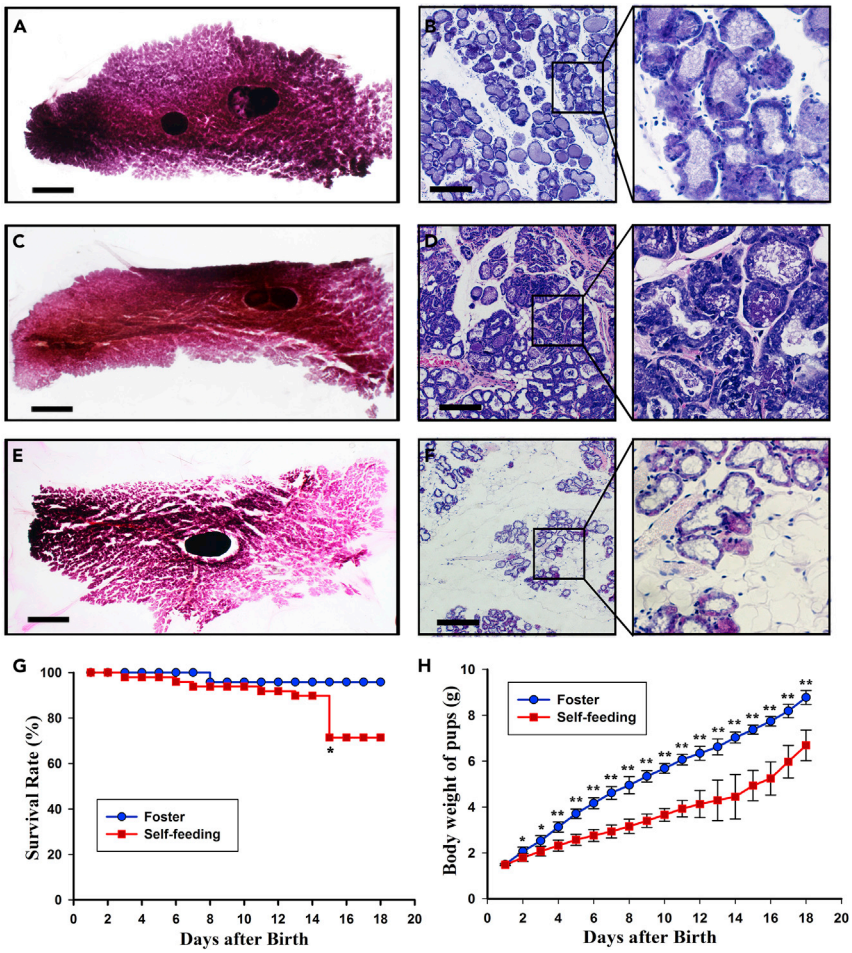

Figure 6. Loss of CDO Resulted in Reduction of Mammary Alveolar and Lactation Insufficiency

(A-F) Whole mount of mammary gland at lactation day 7 (L7) of (A) WT (n=4), (C) CSAD KO (n=4), and (E) CDO KO (n=4) mice. Scale bar represents 5mm. Mircro-structure of mammary gland at L7 of (B) WT, (D) CSAD KO, and (F) CDO KO mice, performed by paraffin section and HE staining.

(G) Survival rate of the offspring from CDO KO mothers during suckling period by foster (n = 24) or self-feeding (n = 49). * represents significant difference of survival rate between CDO KO mother self-feeding offspring and foster offspring (χ^2 test, p = 0.0269).

(H) Growth curve of the offspring of CDO KO mother during suckling period by foster (n = 24) or self-feeding (n = 49). Significant difference of body weight between CDO KO mother self-feeding offspring and foster offspring marked with * (t test, *p < 0.05, **p < 0.01).

CDO deletion will lead to deficiency of CSA and taurine along with cysteine accumulation in the cells (Jurkowska et al., 2014; Stipanuk et al., 2006, 2009; Ueki et al., 2011). We hypothesized that mammary dysplasia in CDO KO mice may be caused by CSA and taurine deficiencies or cysteine toxicity. We attempted to create intracellular cysteine excess by cysteine-Cl supplementation (200 mg/kg body weight) via intraperitoneal (i.p.) injection once a day (q.d.) or by 0.5% (w/v) cysteine-Cl supply in drinking water from 21 days postpartum (P21) to P41 in WT mice. We also supplemented the CDO KO mice with CSA (50 or 100 mg/kg body weight) or taurine (100 mg/kg body weight) from P21 to P41 q.d. via i.p. injection. Equal volume (10 mL/kg body weight) of NaCl solution (0.8% w/v) was injected q.d. into WT and CDO KO females as control. After 21-day treatment, their fourth mammary glands were collected and whole-mount analysis was performed. The results showed that neither injection nor supplementation of cysteine-Cl in drinking water showed obvious impact on mammary ductal development in WT mice (Figures 7D, 7E, 7G–7I, and S5). In contrast, CSA supplementation promoted mammary ductal elongation and branching in a dose-dependent manner (Figures 7J–7L and 7N–7P). The ductal branching morphogenesis can be almost restored in CDO KO mice when treated with CSA at a dose of 100 mg/kg body weight (Figures 7L and

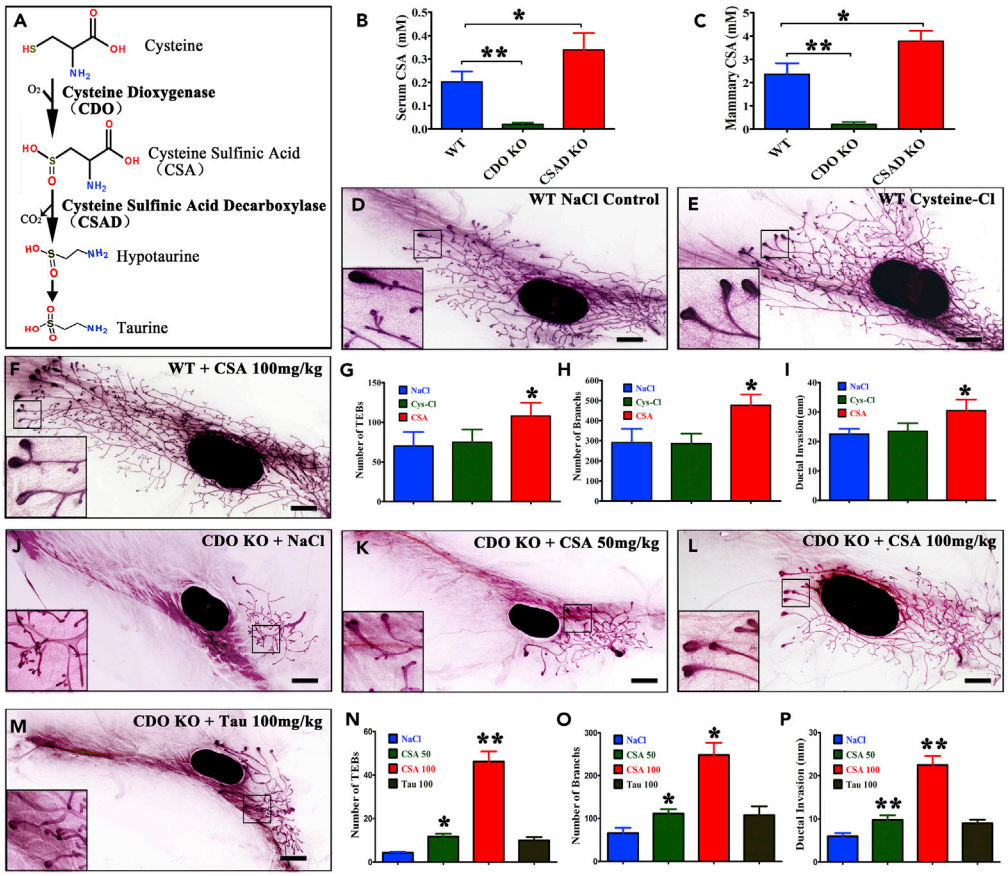

Figure 7. CSA Supplementation Rescues Mammary Duct Branching Morphogenesis of CDO KO Mice

(A) Pathway of cysteine oxidative metabolism.

(B) Serum CSA level of WT (n = 4), CDO KO (n = 4), and CSAD KO (n = 4) mice assayed by high-performance liquid chromatography. CDO KO mice showed significant reduction of serum CSA compared with WT (0.02 ± 0.007 versus 0.202 ± 0.044 mM) (t test, t-value = 7.342, p = 0.005) and CSAD KO mice showed increased serum CSA compared with WT (0.339 ± 0.072 versus 0.202 ± 0.044 mmol/L) (t test, t-value = −5.717, p = 0.011).

(C) CSA levels in mammary tissue of WT (n = 4), CDO KO (n = 4), and CSAD KO (n = 4) mice. Similar to serum level, CSA was deficient in CDO KO mammary, but increased in CSAD KO mammary (WT 2.37 ± 0.467, CDO KO 0.21 ± 0.097, CSAD KO 3.79 ± 0.434 mmol/kg) (WT versus CDO KO, t test, t-value = 7.713, p = 0.005; WT versus CSAD KO, t test, t-value = −4.212, p = 0.024).

(D–F and J–M) The fourth mammary whole mount from 42-day-old WT or CDO KO mice with different treatments from P21 to P41. (D) Mammary collected from WT mice supplemented with 0.8% (w/v) NaCl (10 mL/kg body weight/day) as a control (n = 4). (E) Mammary collected from WT mice supplemented with cysteine-Cl (200 mg/kg body weight/day i.p.) (n = 4). (F) Mammary collected from WT female supplemented with CSA (100 mg/kg body weight i.p. q.d.) (n = 4). (J) Mammary collected from CDO KO mice supplemented with 0.8% NaCl (10 mL/kg body weight/day i.p.) as a control (n = 4). (K) Mammary collected from CDO KO mice supplemented with CSA (50 mg/kg body weight/day i.p.) (n = 4). (L) Mammary collected from CDO KO mice supplemented with CSA (100 mg/kg body weight/day i.p.) (n = 4). (M) Mammary collected from CDO KO mice supplemented with taurine (100 mg/kg body weight/day i.p.) (n = 4).

(G–I) Influence of cysteine-Cl and CSA supplementation on (G) TEB number (t test, NaCl versus CSA, t-value = −3.196, p = 0.049), (H) ductal branch number (t test, NaCl versus CSA, t-value = −3.836, p = 0.031), and (I) ductal invasion length (t test, NaCl versus CSA, t-value = −3.411, p = 0.042) of WT mice mammary gland (the quantitative analysis of B–D).

(N–P) Influence of CSA and taurine supplementation on (N) TEB number (t test, NaCl versus CSA 50, t-value = −7.687, p = 0.025; NaCl versus CSA100, t-value = −9.276, p = 0.003; NaCl versus Tau100, t-value = −2.777, p = 0.069), (O) ductal invasion length (t test, NaCl versus CSA 50, t-value = −3.932, p = 0.029; NaCl versus CSA100, t-value = −5.342, p = 0.031; NaCl versus Tau100, t-value = −2.906, p = 0.062), and (P) ductal branch number (t test, NaCl versus CSA 50, t-value = −7.000, p = 0.006; NaCl versus CSA100, t-value = −6.755, p = 0.007; NaCl versus Tau100, t-value = −2.333, p = 0.102) of CDO KO mice mammary gland (the quantitative analysis of J–M). Scale bar, 2 mm. * represents significant difference compared with control (t test, p < 0.05), ** represents significant difference compared with control (t test, p < 0.01).

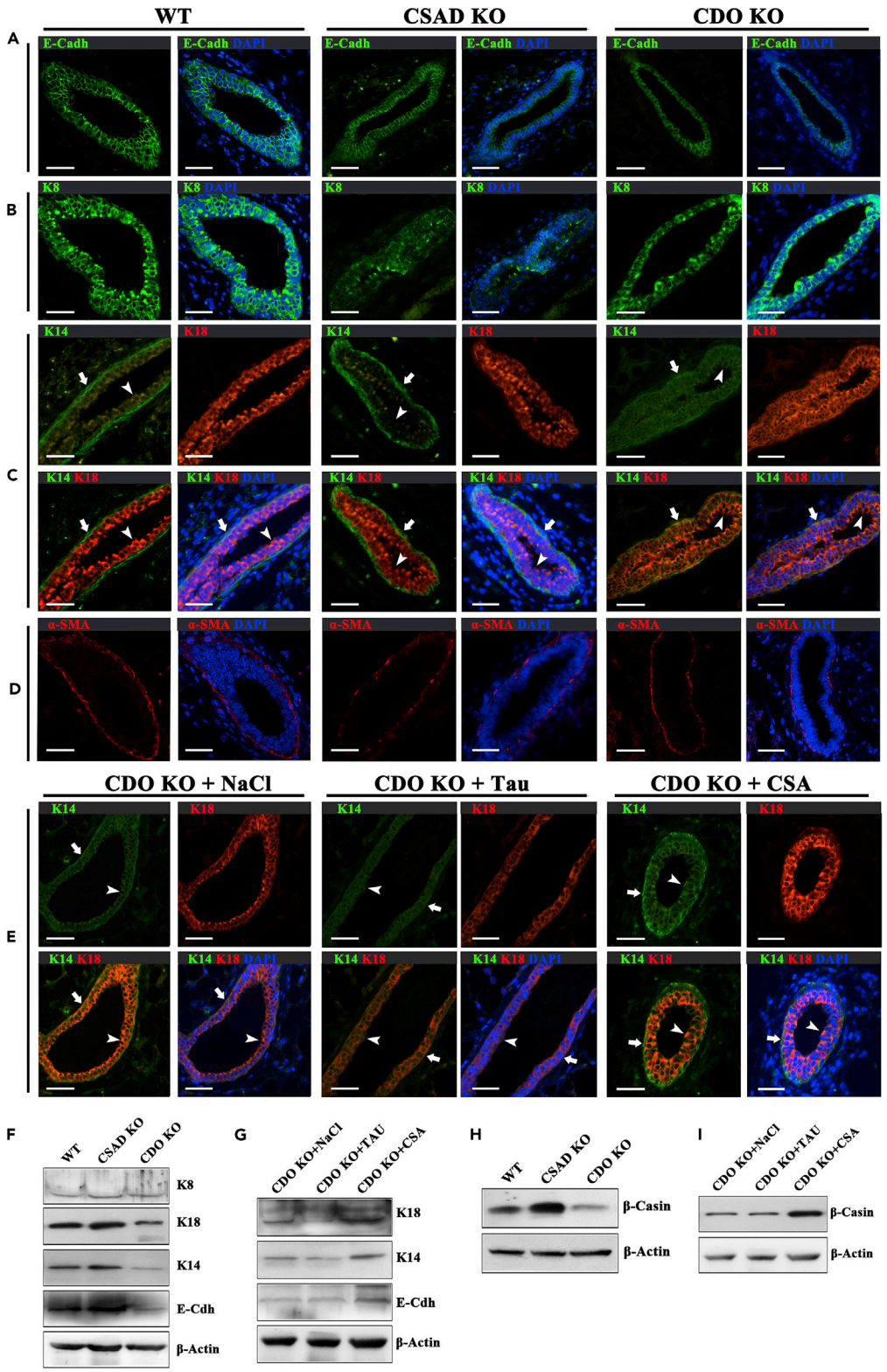

Figure 8. CDO Loss Changed Luminal Cell Character

(A) Immunostaining of E-cadherin (E-Cadh) in WT, CSAD KO, and CDO KO mammaries (n = 4).

(B) Immunostaining of keratin 8 (K8) in WT, CSAD KO, and CDO KO mammaries (n = 4).

Figure 8. *Continued*

(C) Co-immunostaining with the luminal epithelial cell marker keratin 18 (K18) and the myoepithelial marker keratin 14 (K14) in WT, CSAD KO, and CDO KO mammaries (n = 4). White coarse arrowhead points to myoepithelium, and white speculate arrowhead points to luminal epithelium (n = 4).

(D) Immunostaining of α-smooth muscle actin (α-SMA) in WT, CSAD KO, and CDO KO mammaries (n = 4).

(E) Co-immunostaining with K18 and K14 in CDO KO mice mammary gland supplemented with NaCl, taurine, or CSA (n = 4). White coarse arrowhead points to myoepithelium, and white speculate arrowhead points to luminal epithelium.

(F) Relative expression of E-Cdh, K8, K18, and K14 proteins in WT, CSAD KO, and CDO KO mammaries (n = 4).

(G) Influence of taurine and CSA supplementation on E-Cdh, K18, and K14 protein levels of CDO KO mice mammary gland (n = 4).

(H) Relative expression of β-casein protein in WT, CSAD KO, and CDO KO mammaries (n = 4).

(I) Influence of taurine and CSA supplementation on β-casein protein level of CDO KO mice mammary gland (n = 4). Scale bar, 50 μm.

7N–7P). Taurine showed little influence on ductal elongation and branching (Figures 7M–7P). All mice injected with excess dosage of CSA (200 mg/kg body weight) became unhealthy and died within 2 weeks of treatment, indicating that CSA can be toxic. In addition, whole-mount analysis of CSAD KO mammary revealed that lack of taurine had little influence on mammary ductal branching morphogenesis (Figure 4B), consistent with our data that taurine supplementation did not restore the mammary ductal branching morphogenesis of CDO KO mice. CSA supplementation also promoted mammary development in WT mice (Figures 7F–7I). All these results suggested that CSA may be the key molecule through which CDO regulates mammary gland development.

CDO Plays a Role in Retaining Lumen Character and Maintaining Luminal Cell Differentiation

To characterize the consequences of CDO deletion in the pubertal mammary gland, we immunostained the mammary glands with luminal epithelial and myoepithelial cell markers. The results showed that positive signals of luminal epithelial-cell-specific marker keratin 8 (K8) and E-cadherin (E-Cadh) located in mammary luminal epithelial cells, and it appeared that no distinct difference was observed among WT, CSAD KO, and CDO KO mammaries (Figures 8A and 8B). Co-immunostaining with the luminal epithelial cell marker keratin 18 (K18) and the myoepithelial marker keratin 14 (K14) revealed that luminal epithelial cells were exclusively K18 positive in all three types of mammary. K14 was exclusively present in myoepithelial cells of WT and CSAD KO mammary. However, in CDO KO mammary, K14 was present not only in myoepithelial cells but also in luminal cells with relatively weaker signal (Figure 8C). It suggested that loss of CDO leads to the luminal cell showing certain characteristics of myoepithelial cells. To clarify whether the luminal cells were transduced into myoepithelial cell in CDO KO mammary, the myoepithelial cell characteristic protein α-smooth muscle actin (α-SMA) was further detected. It revealed that α-SMA was distinctively expressed in myoepithelium and was negative in luminal epithelial cells in all three types of mammaries (Figure 8D). CSA supplementation increased K14 expression slightly in myoepithelial cells, but reduced K14 expression in luminal epithelial. Taurine supplementation had little effect on K14 expression (Figure 8E). CSA and taurine supplementation had no effect on α-SMA distribution (Figure S6). In addition, estrogen receptor alpha (ERα) distribution in luminal epithelium showed no difference among three genotypes of mice (Figure S7).

To verify these findings, we compared the relative expression of these proteins by WB. The results indicated that luminal marker K18 and E-Cadh and myoepithelium marker K14 decreased in CDO KO mammary, but increased in CSAD KO mammary (Figure 8F). CSA, not taurine supplementation, to CDO KO mice increased the relative expression of K18, E-Cadh, and K14 (Figure 8G).

Relative expression of β-casein was determined to assess the luminal epithelial differentiation in the mammary of the three genotypes of mice by WB. Similarly, loss of CDO led to a relative reduction of β-casein, but loss of CSAD increased β-casein (Figure 8H). CSA supplementation restored the expression of β-casein (Figure 8I).

Our results suggested that CDO in the mammary plays a role in retaining lumen character and maintaining luminal cell differentiation via CSA, which is accumulated in CSAD KO mice, but deficient in CDO KO mice.

Loss of CDO Disturbs Cell Proliferation and Cell Apoptosis

To reveal the mechanism behind the reduction and validity of epithelial cell in CDO KO mammary, we analyzed cell proliferation and cell death of 6-week-old mouse mammary. Ki67 was immunostained to mark proliferating cells, and TUNEL (terminal-deoxynucleotidyl transferase-mediated dUTP nick end

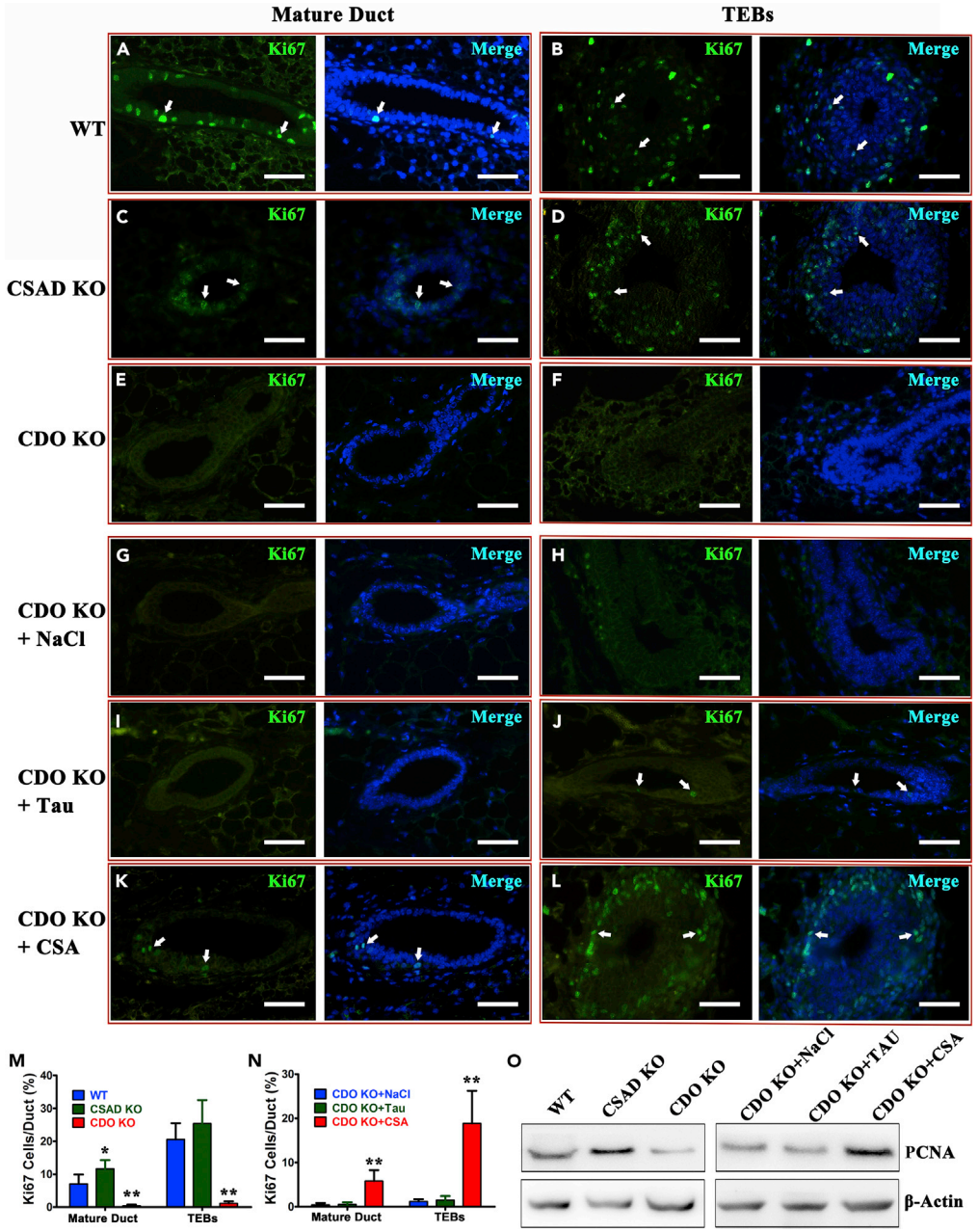

Figure 9. Loss of CDO Resulted in Reduction of Epithelial Cell Proliferation in Mammary Gland, which Was Rescued by CSA Supplementation

(A, C, and E) Ki67 label in mature ducts of (A) WT, (C) CSAD KO, and (E) CDO KO mammary glands (n = 4 mammary per treatment).

(B, D, and F) Ki67 label in TEBs of (B) WT, (D) CSAD KO, and (F) CDO KO mammary glands (n = 4 mammary per treatment).

(G, I, and K) Ki67 label in mature ducts of CDO KO mice mammary gland with (G) NaCl, (I) taurine, or (K) CSA supplementation (n = 4 mammary per treatment).

(H, J, and L) Ki67 label in TEBs of CDO KO mice mammary gland with (H) NaCl, (J) taurine, or (L) CSA supplementation (n = 4 mammary per treatment). White arrows point to Ki67-positive cells' stain in green or merge with DAPI stain, which represents proliferating cells. Scale bar, 50 μm.

(M–O) (M) Quantification of Ki67-positive cell percentage in mature ducts and TEBs of WT (n = 4), CSAD KO (n = 4), and CDO KO (n = 4) mammaries. Two different sections were obtained in one sample, and at least three ducts per section were counted to calculate the percentage of Ki67-positive cells in mammary ducts. CSAD KO mammary showed more Ki67-positive cells in mature ducts than WT (WT versus CSAD KO, t test, t-value = −2.69, p = 0.045). CDO KO mammary

Figure 9. *Continued*
showed significant decrease in Ki67-positive cells both in mature ducts and TEBs compared with WT (WT versus CDO KO, mature duct: t test, t-value = 5.542, p = 0.003; TEBs: t test, t-value = 9.477, p = 0.000). (N) Quantification of Ki67-positive cell percentage in mature ducts and TEBs of CDO KO mice mammary supplemented with NaCl, taurine, or CSA. CSA supplementation significantly enhanced cell proliferation both in mature ducts and TEBs (NaCl versus CSA, mature duct: t test, t-value = −5.015, p = 0.004; TEBs: t test, t-value = −5.977, p = 0.002) (O) PCNA levels in WT and KO mice and CDO KO mice supplemented with NaCl, taurine, or CSA. * represents significant difference compared with WT ($p < 0.05$), ** represents significant difference compared with control ($p < 0.01$).

labeling) examination was used to label apoptotic cells. The results indicated that loss of CDO led to extreme reduction both in cell proliferation and cell death rate in mature ducts and TEBs (Figures 9A, 9B, 9E, 9F, 9M, 10A–10C, and 10G). To the contrary, loss of CSAD stimulated cell proliferation in mature ducts (Figures 9A–9D and 9M) and maintained cell death (Figures 10A–10C and 10G). When supplemented with CSA, Ki67-positive cells significantly increased in mature duct and TEBs (Figures 9G, 9H, 9K,9L, and 9N), whereas taurine supplementation showed little effect(Figures 9G–9J, and 9N). Proliferating cell nuclear antigen protein levels, which were detected using WB of mammary lysate, were maintained in accordance with Ki67 (Figure 9O). Similarly, CSA supplementation to CDO KO females partially rescued the cell death rate (Figures 10D–10F and 10H). Taurine supplementation showed little effect (Figures 10D–10F and 10H). These data indicated that CDO plays an important role in regulating cell homeostasis and renewal via CSA and consequently contributes to epithelial morphogenesis in the mammary gland.

DISCUSSION

In this study, we discovered that CDO, a key enzyme in cysteine oxidative metabolism and taurine biosynthesis, regulates mammary epithelial morphogenesis through its direct downstream metabolite CSA. It has been reported that the offspring of CDO KO females could not survive; however, the mechanism is unknown (Ueki et al., 2011). Mammary epithelial morphogenesis is the base of organotypic growth of mammary parenchyma and important for functional formation (Macias and Hinck, 2012; Nelson et al., 2006; Watson and Khaled, 2008). As we know, mammary gland development is a complex process with a variety of statuses in different developmental stages. In this study, we initially found that CDO was enriched in the mammary gland of branching morphogenesis stages, but was lacking in alveolus stages. We confirmed that loss of CDO led to severe defects in mammary branching morphogenesis, ductal elongation, and poor lactation outcome. We provided evidence that the death of the offspring resulted from the insufficient lactation of CDO KO mothers.

Mammary branching morphogenesis and elongation are predominantly active after onset of puberty, which largely depends on pituitary and ovarian hormones, such as GH, PRL, estrogen, and progesterone (LaMarca and Rosen, 2008; Watson and Khaled, 2008). Our data indicated that CDO is abundant in virgin mammary gland, but is very little in endocrine organs including hypothalamus, pituitary, and ovary. Adult CDO KO females are fertile, and pituitary produced GH and PRL properly in CDO KO females. The results of our mammary-gland-specific CDO expression and KO experiments suggest that the process of CDO regulating mammary development is independent of pituitary and ovarian endocrine action.

In this work, we revealed a novel role for CDO in regulating mammary ductal epithelial morphogenesis and lactation function. In addition, it is interesting that CDO is enriched in typical tree-like developmental organs including mammary gland, lung, and kidney, implying that it may be a common factor in regulating the organ branching morphogenesis and functional formation. We also found more large alveoli in the lung of adult CDO KO mice, resulting in decreased alveolar surface area. It may be a consequence of insufficient lung branching morphogenesis.

CDO and CSAD are rate-limiting enzymes in taurine synthesis. Both CDO KO mice and CSAD KO mice exhibited systematic taurine deficiency. However, CSAD KO females did not show the defect in mammary development. On the contrary, CSAD KO mammary possessed more milk production alveolar unit compared with WT mice during lactation stage. It suggests that taurine is not the key molecule that supports mammary development. In this work, we provide evidences that CSA greatly rescued the mammary dysplasia resulting from loss of CDO and that it also significantly contributed to mammary ductal growth in WT mice. CSA is the direct downstream product of CDO, and it is also the substrate of CSAD (Peck and Awapara, 1967; Singer and Kearney, 1954). Therefore loss of CDO led to CSA deficiency, but loss of CSAD resulted in CSA accumulation in cells. It was confirmed by both serum and mammary CSA assays.

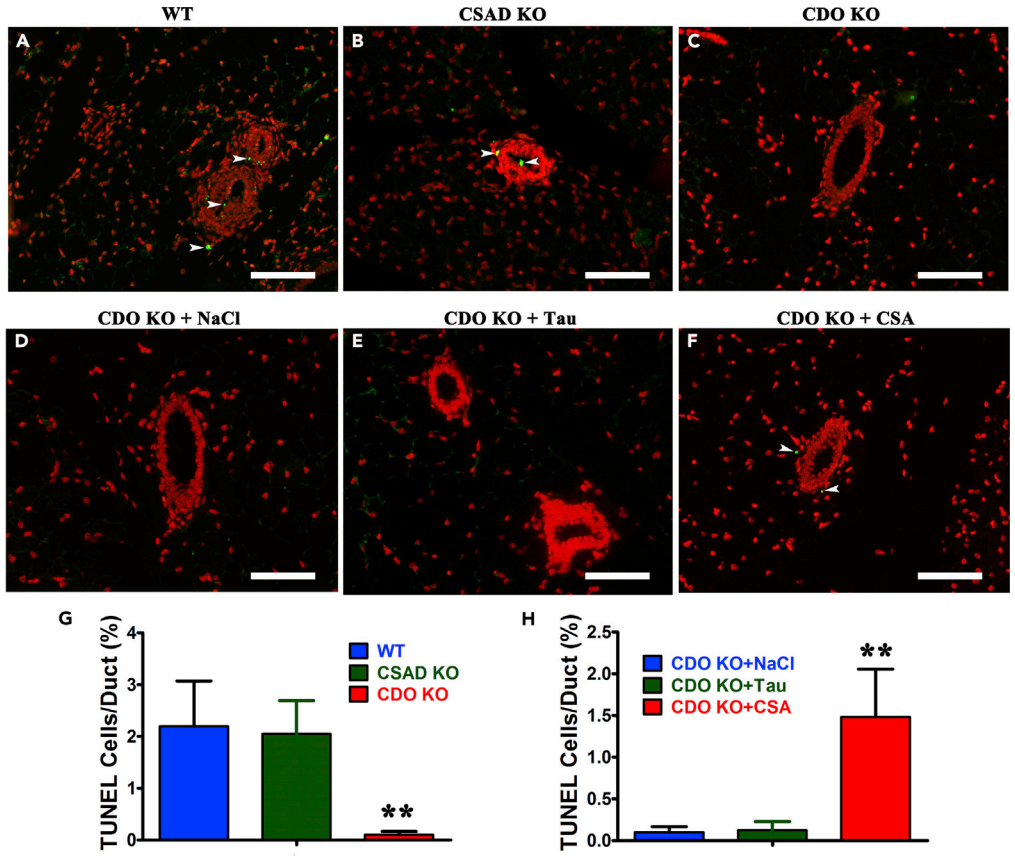

Figure 10. Loss of CDO Led to Reduction of Cell Death in Mammary Gland

TUNEL signals (green) were merged with cell nucleus (Propidium iodide staining in red).

(A–C) Cell death in mature ducts of (A) WT, (B) CSAD KO, and (C) CDO KO mammary glands (n = 4 mammary per treatment).

(D–F) Cell death in mature ducts of CDO KO mice mammary gland with (D) NaCl, (E) taurine, or (F) CSA supplementation (n = 4 mammary per treatment). White arrow points to TUNEL-positive cells, which represents apoptotic cells. Scale bar, 100 μm.

(G) Quantification of TUNEL-positive cell percentage in mature ducts of WT (n = 4), CSAD KO (n = 4), and CDO KO (n = 4) mammaries. CDO KO mammary showed significant decrease in TUNEL-positive cells in mature ducts compared with WT (WT versus CDO KO, t test, t-value = 5.774, $p = 0.002$).

(H) Quantification of TUNEL-positive cell percentage in mature ducts of CDO KO mice mammary supplemented with NaCl, taurine, or CSA. CSA supplementation significantly rescued cell apoptosis in mature ducts (NaCl versus CSA, t test, t-value = −6.132, $p = 0.002$). ** represents significant difference compared with WT or control ($p < 0.01$).

Our results showed that loss of CSAD exhibited an effect similar to CSA supplementation. Known as a precursor of taurine biosynthesis, CSA has been described to exist in the central nervous system as a neurotransmitter (Baba et al., 1982; Recasens et al., 1982). CSA is able to enter and exit from cells through interaction with special receptors on the cell membrane (Abele et al., 1983; Iwata et al., 1982; Recasens et al., 1983). However, understanding of the biological functions of CSA is still rather limited. Here, we provide evidences that CSA has positive effect on promoting mammary gland development, which would be a potential solution for mammary dysplasia in human and farm animals.

Mammary gland has been utilized to study the general mechanisms of epithelial morphogenesis as well as to understand the more pressing issue of mammary tumorigenesis (Daniel and Smith, 1999; Howlin et al., 2006; Medina, 1996). The increased incidence of breast tumors in nulliparous women may be related to the low degree of differentiation of mammary epithelial cells (Russo et al., 2005). Here we showed that the CDO is an important regulator maintaining luminal epithelium character and luminal epithelial cell differentiation via CSA in the mammary gland. CDO KO mammary displayed less differentiated luminal epithelial cells with the characteristics of myoepithelium. We have verified that the protein level of epithelial cell markers

decreased in CDO KO mammary, which can be upregulated by CSA. β-casein, a luminal epithelial differentiation marker, reduced in CDO KO mammary, which can be upregulated by CSA. Recent studies have revealed that CDO inactivation is associated with the occurrence of various cancers (Brait et al., 2012; Jeschke et al., 2013). Loss of organization is associated with cancer (Chanson et al., 2011). In addition, we showed a disorganized epithelium in mammary ducts and higher risk of developing breast tumors in CDO KO mice older than 12 weeks. It suggests that CDO has an important role in maintaining lumen and epithelial cell differentiation via CSA, which has important implications for epithelial cell fate determination and pathogenesis of breast cancer.

Mammary development involves epithelial cell proliferation and apoptosis. After onset of puberty, mammary development is driven by the highly proliferative TEBs, which actuate ductal elongation and branching in the surrounding fat pad until the ducts reach the edge limits of the fat pad (Howlin et al., 2006; Nelson et al., 2006; Owens et al., 1973). Epithelial cell apoptosis is vital in mammary development and functional formation (Green and Streuli, 2004; Humphreys et al., 1996). In the present study, we showed evidences that CDO maintained both levels of epithelial cell proliferation and apoptosis. Importantly, loss of CDO dramatically reduced both cell proliferation and apoptosis. The unregulated processes of cell proliferation and apoptosis can be rescued by CSA supplementation, which has an implication in organ regeneration and cell renewal.

In conclusion, our study demonstrated that CDO plays important roles in regulating mammary epithelial cell differentiation, proliferation, and apoptosis, through which mammary epithelial morphogenesis is controlled. Importantly, instead of taurine, the direct downstream metabolite of CDO CSA was heavily involved in these processes. Our findings have led to appreciative discovery of the relationship between cysteine metabolism and mammary epithelial morphogenesis and have provided insights into the organ morphogenesis and implications in tumorigenesis.

Limitations of the Study

In this study we described that CDO regulates mammary epithelial morphogenesis via CSA, which maintains epithelial cell differentiation, proliferation, and apoptosis. However, the mechanisms of CSA's action are not fully demonstrated in this study. Our data suggest that CDO may be a common factor in regulating the organ branching morphogenesis and functional formation. However, these inferences need more experiments to be clarified.

METHODS

All methods can be found in the accompanying Transparent Methods supplemental file.

SUPPLEMENTAL INFORMATION

Supplemental Information can be found online at https://doi.org/10.1016/j.isci.2019.02.011.

ACKNOWLEDGMENTS

We thank Dr. Hefang Xie for her valuable comments on our manuscript. This work was supported by Chongqing Research Program of Basic Research and Frontier Technology (cstc2016jcyjA0386), Fundamental Research Funds for the Central Universities (XDJK2016C050), Fundamental Research Funds for the Central Universities (No.XDJK2018B024), and Doctoral Funds of Southwest University (2016).

AUTHOR CONTRIBUTIONS

J.Z., and A.L. conceived this study. J.Z and Y. H. designed the experiments. J.Z., X.M., G.Y., H.L., P.F., and B.Q. performed the experiments. Y.Z, S.Y, Q.S, and G.Z analyzed the data. J.Z., Y.Z, and Q.S. wrote the manuscript.

DECLARATION OF INTERESTS

A patent application has been filed related to this work. The authors declare no competing interests.

Received: August 9, 2018
Revised: February 11, 2019
Accepted: February 13, 2019
Published: March 29, 2019

REFERENCES

Abele, A., Borg, J., and Mark, J. (1983). Cysteine sulfinic acid uptake in cultured neuronal and glial cells. Neurochem. Res. *8*, 889–902.

Baba, A., Lee, E., Tatsuno, T., and Iwata, H. (1982). Cysteine sulfinic acid in the central nervous system: antagonistic effect of taurine on cysteine sulfinic acid-stimulated formation of cyclic AMP in Guinea pig hippocampal slices. J. Neurochem. *38*, 1280–1285.

Brait, M., Ling, S., Nagpal, J.K., Chang, X., Park, H.L., Lee, J., Okamura, J., Yamashita, K., Sidransky, D., and Kim, M.S. (2012). Cysteine dioxygenase 1 is a tumor suppressor gene silenced by promoter methylation in multiple human cancers. PLoS One *7*, e44951.

Chanson, L., Brownfield, D., Garbe, J.C., Kuhn, I., Stampfer, M.R., Bissell, M.J., and LaBarge, M.A. (2011). Self-organization is a dynamic and lineage-intrinsic property of mammary epithelial cells. Proc. Natl. Acad. Sci. U S A *108*, 3264–3269.

Daniel, C.W., and Smith, G.H. (1999). The mammary gland- a model for development. J. Mammary Gland Biol. Neoplasia *4*, 3–8.

Debnath, J., Mills, K.R., Collins, N.L., Reginato, M.J., Muthuswamy, S.K., and Brugge, J.S. (2002). The role of apoptosis in creating and maintaining luminal space within normal and oncogene-expressing mammary acini. Cell *111*, 29–40.

Driggers, C.M., Cooley, R.B., Sankaran, B., Hirschberger, L.L., Stipanuk, M.H., and Karplus, P.A. (2013). Cysteine dioxygenase structures from pH4 to 9: consistent cys-persulfenate formation at intermediate pH and a Cys-bound enzyme at higher pH. J. Mol. Biol. *425*, 3121–3136.

Gordon, C., Bradley, H., Waring, R.H., and Emery, P. (1992). Abnormal sulphur oxidation in systemic lupus erythematosus. Lancet *339*, 25–26.

Green, K.A., and Streuli, C.H. (2004). Apoptosis regulation in the mammary gland. Cell Mol. Life Sci. *61*, 1867–1883.

Heafield, M.T., Fearn, S., Steventon, G.B., Waring, R.H., Williams, A.C., and Sturman, S.G. (1990). Plasma cysteine and sulphate levels in patients with motor neurone, Parkinson's and Alzheimer's disease. Neurosci. Lett. *110*, 216–220.

Hennighausen, L., and Robinson, G.W. (2005). Information networks in the mammary gland. Nat. Rev. Mol.Cell Biol. *6*, 715–725.

Howlin, J., McBryan, J., and Martin, F. (2006). Pubertal mammary gland development: insights from mouse models. J. Mammary Gland Biol. Neoplasia *11*, 283–297.

Huebner, R.J., and Ewald, A.J. (2014). Cellular foundations of mammary tubulogenesis. Semin.Cell Dev. Biol. *31*, 124–131.

Humphreys, R.C., Krajewska, M., Krnacik, S., Jaeger, R., Weiher, H., Krajewski, S., Reed, J.C., and Rosen, J.M. (1996). Apoptosis in the terminal endbud of the murine mammary gland: a mechanism of ductal morphogenesis. Development *122*, 4013–4022.

Iwata, H., Yamagami, S., and Baba, A. (1982). Cysteine sulfinic acid in the central nervous system: specific binding of [35S]cysteic acid to cortical synaptic membranes–an investigation of possible binding sites for cysteine sulfinic acid. J. Neurochem. *38*, 1275–1279.

Jeschke, J., O'Hagan, H.M., Zhang, W., Vatapalli, R., Calmon, M.F., Danilova, L., Nelkenbrecher, C., Van Neste, L., Bijsmans, I.T., Van Engeland, M., et al. (2013). Frequent inactivation of cysteine dioxygenase type 1 contributes to survival of breast cancer cells and resistance to anthracyclines. Clin. Cancer Res. *19*, 3201–3211.

Joseph, C.A., and Maroney, M.J. (2007). Cysteine dioxygenase: structure and mechanism. Chem. Commun. (Camb.) *32*, 3338–3349.

Jurkowska, H., Roman, H.B., Hirschberger, L.L., Sasakura, K., Nagano, T., Hanaoka, K., Krijt, J., and Stipanuk, M.H. (2014). Primary hepatocytes from mice lacking cysteine dioxygenase show increased cysteine concentrations and higher rates of metabolism of cysteine to hydrogen sulfide and thiosulfate. Amino Acids *46*, 1353–1365.

Kouros-Mehr, H., Slorach, E.M., Sternlicht, M.D., and Werb, Z. (2006). GATA-3 maintains the differentiation of the luminal cell fate in the mammary gland. Cell *127*, 1041–1055.

LaMarca, H.L., and Rosen, J.M. (2008). Minireview: hormones and mammary cell fate–what will I become when I grow up? Endocrinology *149*, 4317–4321.

Macias, H., and Hinck, L. (2012). Mammary gland development. Wiley Interdiscip. Rev. Dev. Biol. *1*, 533–557.

Mailleux, A.A., Overholtzer, M., and Brugge, J.S. (2008). Lumen formation during mammary epithelial morphogenesis: insights from in vitro and in vivo models. Cell Cycle *7*, 57–62.

McBryan, J., and Howlin, J. (2017). Pubertal mammary gland development: elucidation of in vivo morphogenesis using murine models. Methods Mol. Biol. *1501*, 77–114.

McCoy, J.G., Bailey, L.J., Bitto, E., Bingman, C.A., Aceti, D.J., Fox, B.G., and Phillips, G.N., Jr. (2006). Structure and mechanism of mouse cysteine dioxygenase. Proc. Natl. Acad. Sci. U S A *103*, 3084–3089.

Medina, D. (1996). The mammary gland: a unique organ for the study of development and tumorigenesis. J. Mammary Gland Biol. Neoplasia *1*, 5–19.

Meller, S., Zipfel, L., Gevensleben, H., Dietrich, J., Ellinger, J., Majores, M., Stein, J., Sailer, V., Jung, M., Kristiansen, G., et al. (2016). CDO1 promoter methylation is associated with gene silencing and is a prognostic biomarker for biochemical recurrence-free survival in prostate cancer patients. Epigenetics *11*, 871–880.

Musumeci, G., Castrogiovanni, P., Szychlinska, M.A., Aiello, F.C., Vecchio, G.M., Salvatorelli, L., Magro, G., and Imbesi, R. (2015). Mammary gland: from embryogenesis to adult life. Acta Histochem. *117*, 379–385.

Nelson, C.M., Vanduijn, M.M., Inman, J.L., Fletcher, D.A., and Bissell, M.J. (2006). Tissue geometry determines sites of mammary branching morphogenesis in organotypic cultures. Science *314*, 298–300.

Owens, I.S., Vonderhaar, B.K., and Topper, Y.J. (1973). Concerning the necessary coupling of development to proliferation of mouse mammary epithelial cells. J. Biol. Chem. *248*, 472–477.

Peck, E.J., Jr., and Awapara, J. (1967). Formation of taurine and isethionic acid in rat brain. Biochim. Biophys. Acta *141*, 499–506.

Ran, F.A., Cong, L., Yan, W.X., Scott, D.A., Gootenberg, J.S., Kriz, A.J., Zetsche, B., Shalem, O., Wu, X., Makarova, K.S., et al. (2015). In vivo genome editing using Staphylococcus aureus Cas9. Nature *520*, 186–191.

Ran, F.A., Hsu, P.D., Lin, C.Y., Gootenberg, J.S., Konermann, S., Trevino, A.E., Scott, D.A., Inoue, A., Matoba, S., Zhang, Y., et al. (2013a). Double nicking by RNA-guided CRISPR Cas9 for enhanced genome editing specificity. Cell *154*, 1380–1389.

Ran, F.A., Hsu, P.D., Wright, J., Agarwala, V., Scott, D.A., and Zhang, F. (2013b). Genome engineering using the CRISPR-Cas9 system. Nat. Protoc. *8*, 2281–2308.

Recasens, M., Saadoun, F., Maitre, M., Baudry, M., Lynch, G., Mandel, P., and Vincendon, G. (1983). Cysteine sulfinate receptors in the rat CNS. Adv. Biochem. Psychopharmacol. *37*, 211–219.

Recasens, M., Varga, V., Nanopoulos, D., Saadoun, F., Vincendon, G., and Benavides, J. (1982). Evidence for cysteine sulfinate as a neurotransmitter. Brain Res. *239*, 153–173.

Russo, J., Moral, R., Balogh, G.A., Mailo, D., and Russo, I.H. (2005). The protective role of pregnancy in breast cancer. Breast Cancer Res. *7*, 131–142.

Schock, F., and Perrimon, N. (2002). Molecular mechanisms of epithelial morphogenesis. Annu. Rev.Cell Dev. Biol. *18*, 463–493.

Shackleton, M., Vaillant, F., Simpson, K.J., Stingl, J., Smyth, G.K., Asselin-Labat, M.L., Wu, L., Lindeman, G.J., and Visvader, J.E. (2006). Generation of a functional mammary gland from a single stem cell. Nature *439*, 84–88.

Simmons, C.R., Liu, Q., Huang, Q., Hao, Q., Begley, T.P., Karplus, P.A., and Stipanuk, M.H. (2006). Crystal structure of mammalian cysteine dioxygenase. A novel mononuclear iron center for cysteine thiol oxidation. J. Biol. Chem. *281*, 18723–18733.

Singer, R.P., and Kearney, E.B. (1954). Pathways of L-cysteinesulfinate metabolism in animal tissues. Biochim. Biophys. Acta *14*, 570–571.

Stipanuk, M.H., Dominy, J.E., Jr., Lee, J.I., and Coloso, R.M. (2006). Mammalian cysteine

metabolism: new insights into regulation of cysteine metabolism. J. Nutr. *136*, 1652S–1659S.

Stipanuk, M.H., Ueki, I., Dominy, J.E., Jr., Simmons, C.R., and Hirschberger, L.L. (2009). Cysteine dioxygenase: a robust system for regulation of cellular cysteine levels. Amino Acids *37*, 55–63.

Ueki, I., Roman, H.B., Valli, A., Fieselmann, K., Lam, J., Peters, R., Hirschberger, L.L., and Stipanuk, M.H. (2011). Knockout of the murine cysteine dioxygenase gene results in severe impairment in ability to synthesize taurine and an increased catabolism of cysteine to hydrogen sulfide. Am. J. Physiol. Endocrinol. Metab. *301*, E668–E684.

Ueki, I., and Stipanuk, M.H. (2007). Enzymes of the taurine biosynthetic pathway are expressed in rat mammary gland. J. Nutr. *137*, 1887–1894.

Van Keymeulen, A., Rocha, A.S., Ousset, M., Beck, B., Bouvencourt, G., Rock, J., Sharma, N., Dekoninck, S., and Blanpain, C. (2011). Distinct stem cells contribute to mammary gland development and maintenance. Nature *479*, 189–193.

Varner, V.D., and Nelson, C.M. (2014). Cellular and physical mechanisms of branching morphogenesis. Development *141*, 2750–2759.

Watson, C.J., and Khaled, W.T. (2008). Mammary development in the embryo and adult: a journey of morphogenesis and commitment. Development *135*, 995–1003.

Williams, J.M., and Daniel, C.W. (1983). Mammary ductal elongation: differentiation of myoepithelium and basal lamina during branching morphogenesis. Dev. Biol. *97*, 274–290.

Ye, S., Wu, X., Wei, L., Tang, D., Sun, P., Bartlam, M., and Rao, Z. (2007). An insight into the mechanism of human cysteine dioxygenase. Key roles of the thioether-bonded tyrosine-cysteine cofactor. J. Biol. Chem. *282*, 3391–3402.

ISCI, Volume *13*

Supplemental Information

Cysteine Dioxygenase Regulates the Epithelial Morphogenesis of Mammary Gland via Cysteine Sulfinic Acid

Jianjun Zhao, Yuzhu Han, Xingyu Ma, Yang Zhou, Shukai Yuan, Qian Shen, Guogen Ye, Hongrun Liu, Penghui Fu, Gongwei Zhang, Bingke Qiao, and Anfang Liu

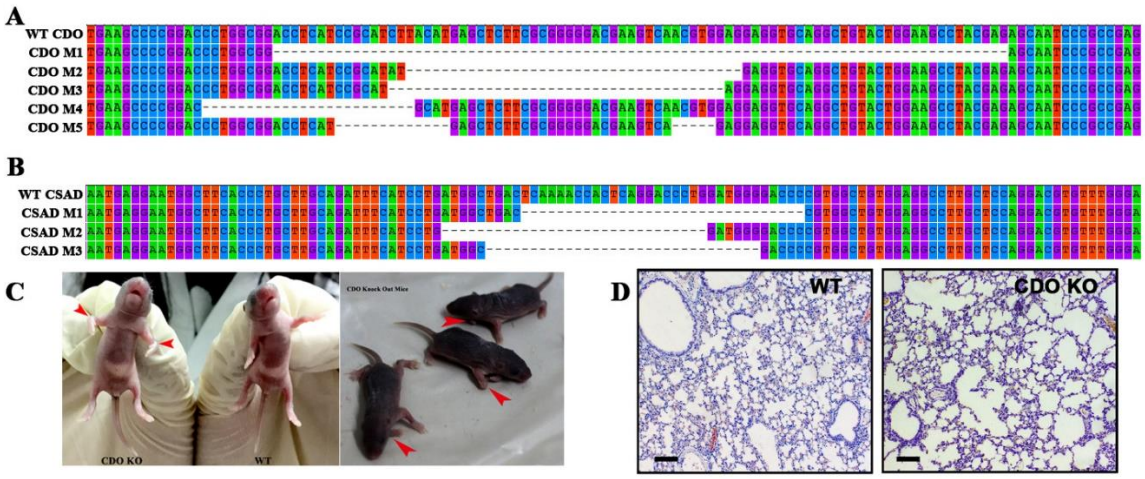

Figure S1 Information of obtained CDO and CSAD mutant lines by CRISPR/Cas9n, related to figure 2 and 3. (A) CDO mutant mice DNA sequence alignment. (B) CSAD mutant mice DNA sequence alignment. (C) CDO KO mice displayed a defect of joint contracture at forelimb. (D) It showed more large alveoli in the lung of adult CDO KO mice compare to WT. Scale bar =100 μm.

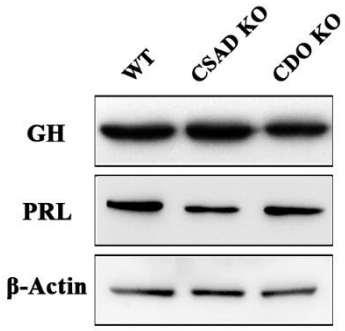

Figure S2 CDO and CSAD had little Influence on syntheses of pituitary growth hormone (GH) and prolactin (PRL), related to figure 4. Western blot of pituitary lysate from WT, CSAD KO, and CDO KO female in 6-week old (n=3 samples each genotype).

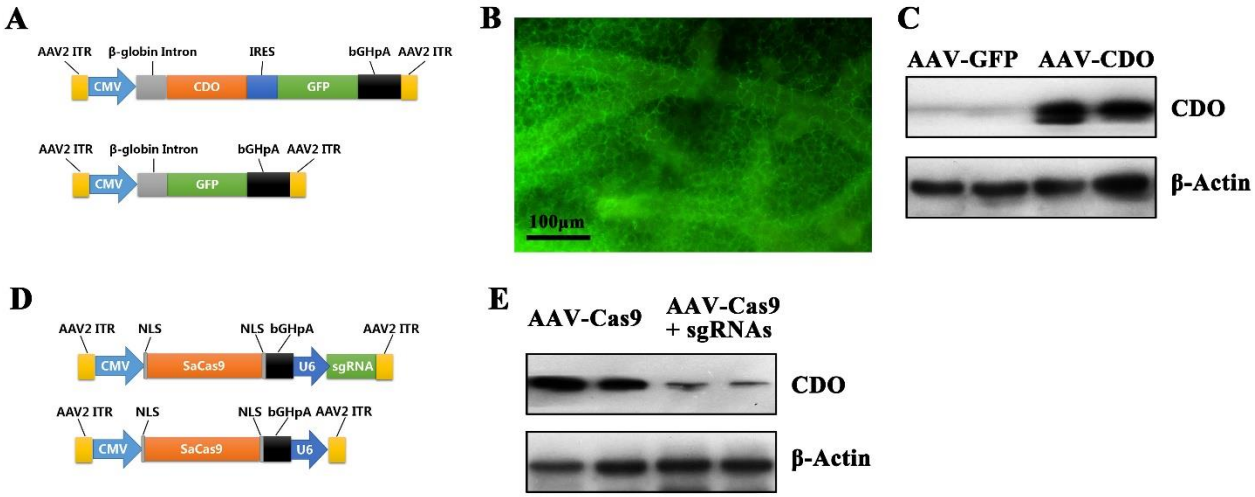

Figure S3 Mammary specific CDO expression and knock out using AAV2, related to figure 4. (A) CDO expression and control AAV vector. CDO coding sequence was cloned into an AAV vector by BamHI and EcoRI double digest which linked a GFP gene by IRES element was driven by a CMV promoter used to packaging CDO expression AAV. An AAV vector of CMV driving GFP was used to package control AAV. (B) AAV mediated GFP expression in mammary gland of CDO KO mice. The CDO expression AAV or GFP AAV was injected into the fourth mammary gland of CDO KO mice at the age of P10 and detected green fluorescence at P24. The mammary gland was spread onto a slide and observed with an inverted fluorescence microscope. (C) CDO expression rescued in CDO KO mice mammary by AAV-CDO delivery vehicle. After 2 weeks from AAV injection, the CDO levels in the mammary were determined using WB. It showed CDO expression in CDO KO mouse mammary were highly rescued by CDO expression AAV injection. (D) pX601 AAV vector with SaCas9 and sgRNA expression cassettes (Addgene plasmid # 61591) constructing with or without a specific guide sequence was used to packaging CDO knock down or control AAVs. (E) For high efficiency of SaCas9 mediated CDO knock out in mammary gland, the AAVs with two high specific SaCas9 targets on mouse CDO were mixed for injection. The CDO Het females were injected with a CDO knock out AAV (SaCas9 with sgRNA) or control AAV (SaCas9 without sgRNA) subcutaneously at the site of the fourth mammary nipple at the age of P10. The CDO expression in the mammary gland was determined after 2 weeks of first injection. It showed significant decrease of CDO expression in the mammary.

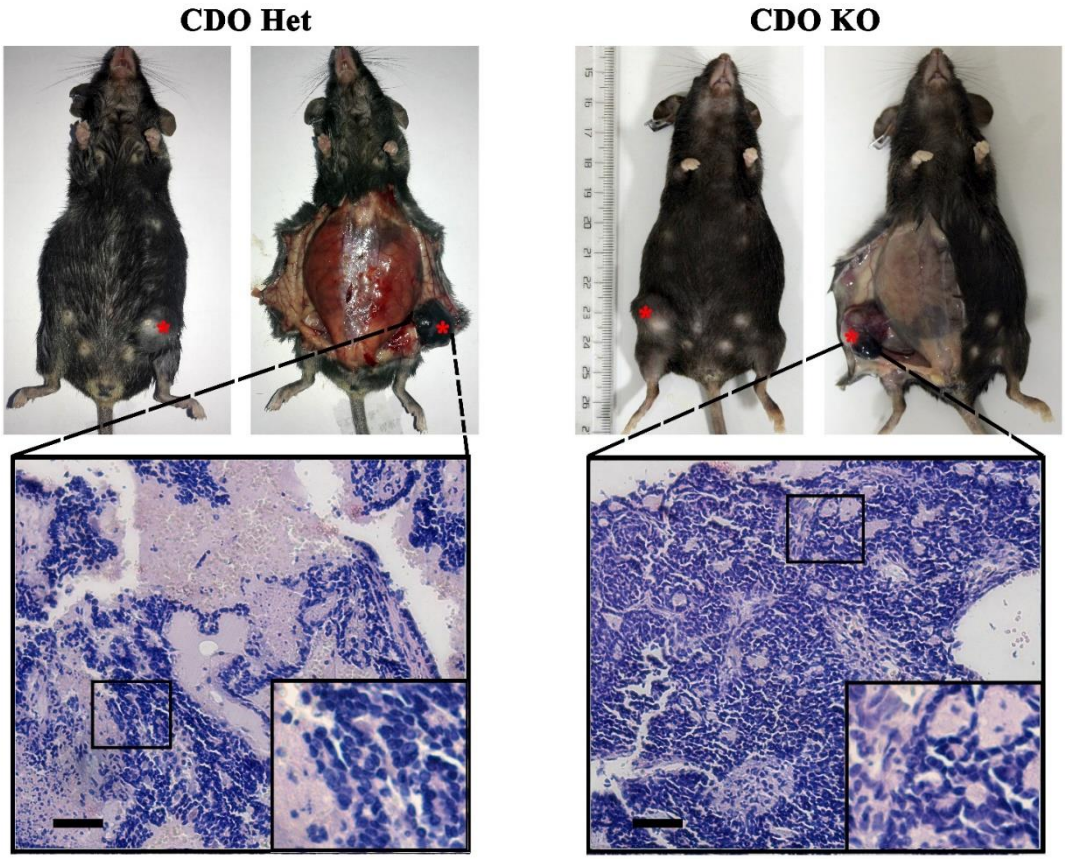

Figure S4 CDO loss result in increased risk of developing breast tumor, related to figure 5 and 8. Cases of CDO heterozygote (CDO Het) and CDO KO mice got breast tumor. Hematoxylin and eosin (HE) staining of paraffin embedded sections of breast tumor. Scale bar =50μm.

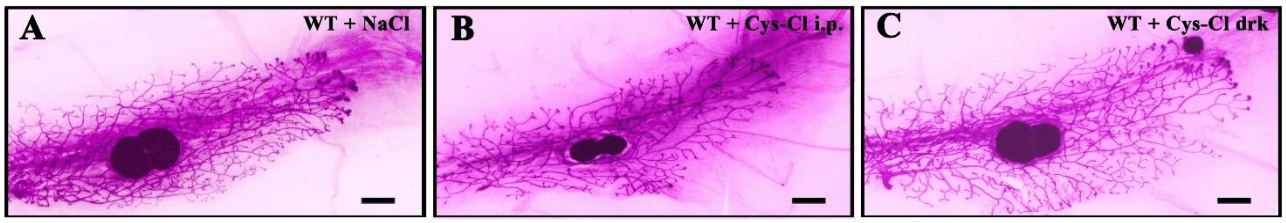

Figure S5 Influence of Cys-Cl supplementation on mammary duct development of WT mice, related to figure 7. The fourth mammary whole mount of 42-day old WT mice with different treatment from P21 to P41. (A) 0.8% NaCl injection control. (B) Cys-Cl injection. (C) Cys-Cl supplementation by drinking water. (n=4 mammary each treatment) Scale bar =2 mm.

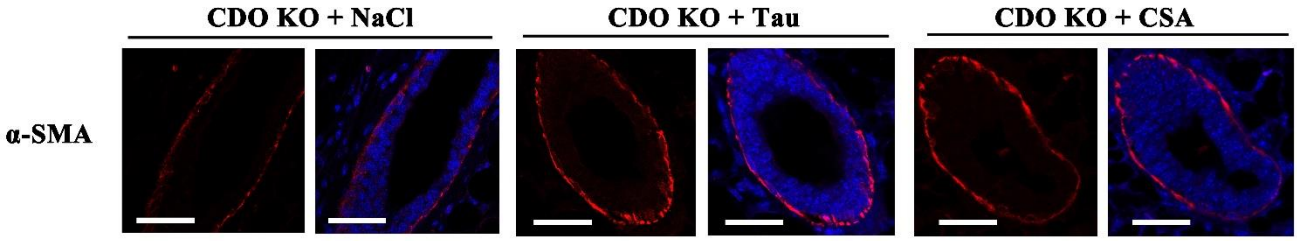

Figure S6 CSA and Taurine have no effect on α-SMA distribution in CDO KO mammary gland, related to figure 8. Scale bar =50μm.

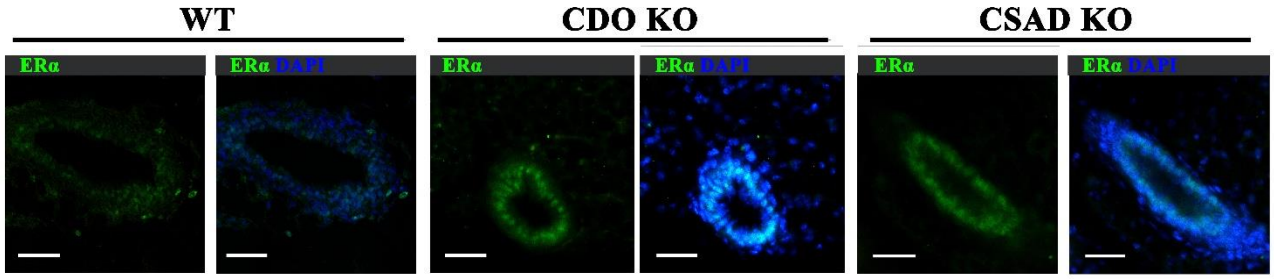

Figure S7 CDO and CSAD have no influence on estrogen receptor distribution in mammary gland, related to figure 8. Scale bar =50μm.

Table S1 Primers for CDO and CSAD mRNA expression assay, related to figure1.

Gene	Primer	Sequence (5'-3')	Product size (bp)
CDO	Forward	TGGAAGCCTACGAGAGCAATCC	181
	Reverse	AGCTTCAGAAAGCAGTGGGAGT	
CSAD	Forward	CATGGAAGAGGAGGTGCTGAAG	311
	Reverse	GAATGATCTGCCTCTCCAGGTC	
β-Actin	Forward	CAGAGCAAGAGAGGTATCCTGAC	206
	Reverse	AAGGTCTCAAACATGATCTGGGT	

Table S2 sgRNA pairs used with SpCas9n to target CDO and CSAD, related to figure 2 and 3.

Gene	Target	Guide sequence (5' to 3')	Length (bp)	PAM
CDO	Left sgRNA	GAAGAGCTCATGTAAGATG	19	CGG
	Right sgRNA	GACGAAGTCAACGTGGAGG	19	AGG
CSAD	Left sgRNA	GCCACGGGGTCCCCATCC	18	AGG
	Right sgRNA	GCCTTGCTCCAGGACGTGTT	20	TGG

Table S3 PCR primers for CDO and CSAD KO mice Determination, related to figure 2 and 3.

Gene	sequence (5' to 3')	product size (bp)
CDO-F	TGTGTGTGGTTGTCTAGCCTG	369
CDO-R	GCGACAGAGAGCTGAAAATCTG	
CSAD-F	GATACTGCCACTGCCCTAATGT	321
CSAD-R	CCAGGAACAGGGATGAACTCAA	

Table S4 Litter size of different mating combination, related to figure 4.

Mate combination		No. of pregnancy female	Duration of pregnancy (day)	Average Litter size	Significance level
Control	WT♂╳WT♀	8	19.5	7.67±1.21	
	WT♂╳Het♀	6	19.5	7.83±1.17	NS
	WT♂╳KO♀	6	19.5	7.83±1.47	NS

NS represents no significant difference with control (t-test).

Table S5 sgRNAs used with SaCas9 to target CDO in mammary, related to figure 4.

Gene	Target	Guide sequence (5' to 3')	Length (bp)	PAM
CDO	sgRNA1	GATGCGGATGAGGTCCGC	18	*CAGGGT*
	sgRNA2	GCCTACGAGAGCAATCCCG	19	*CCGAGT*

Transparent Methods

Animal models. CDO and CSAD gene knockout (KO) mice were generated by CRISPR/Cas9. SpCas9n (D10A) was used in this study, as described previously (Ran et al., 2013a; Ran et al., 2013b), and the guide sequence were truncated for high specificity (Fu et al., 2014). We selected a pair of guide sequence in codon region of the first exon of mouse CDO gene (Table S2), which has no potential off

targets (http://crispr.mit.edu). A pair of guide sequence in codon of the second exon of mouse CSAD as SpCas9n target, which have no potential off target sits (Table S2). The pSpCas9n (D10A) plasmid was a gift from Feng Zhang (Addgene plasmid # 48873). The guide sequence oligoes were synthesized by GeneWiz Corporation (Suzhou China). The sgRNAs and SpCas9n mRNA were synthesized as previous described (Li et al., 2013; Wang et al., 2013). Gene KO mice were generated by micro-injection the mixture of SpCas9n (D10A) mRNA (60 ng/μL) and sgRNAs (25 ng/μL) into cytoplasm of 0.5 dpc (days post coitum) embryos and then transferred to the oviduct of a pseudopregnancy female. The F0 generation mice were genotyped by PCR and Sanger sequencing of target region. CDO heterozygous (CDO Het) mice were crossed to generate CDO KO mice that were homozygous for the CDO KO mutation. Genotype of KO mice were determined by analysis of genomic DNA extracted from tail snips, using a pair of specific primers flanking the CDO mutation region (Table S3). Mice were genotyped at postnatal day 7 (P7) and weaned at day P25. CSAD KO mice were obtained through the same routine as above.

All the animal experiments were approved by the Laboratory Animal Welfare and Ethics Committee of SOUTHWESY UNIVERSITY (P. R. China). The mice were housed at 24±2℃, relative humidity of 55±15%, kept in clean cages under 14–h/10–h light–dark cycle and fed with standard rodent diet throughout the entire experimental period.

Adeno-associated virus (AAV) production and animal injection process

Mouse CDO coding region was cloned into an AAV-IRES-GFP vector with CMV promoter (Figure S5 A) and was used to package CDO expression AAV. An AAV-GFP vector with CMV promoter (Figure S5 A) was used for control. SaCas9 AAV vector pX601 was a gift from Feng Zhang (Addgene plasmid # 61591) (Ran et al., 2015) which was constructed with or without a specific guide sequence to package CDO knock out or control AAVs, respectively (Figure S5 D). We selected two highly specific guide sequences in codon region of the first exon of mouse CDO gene (Table S4) (http://crispor.tefor.net/)(Haeussler et al., 2016). The guide sequences were constructed into pX601 and used to package AAV.

293T cells used in virus packaging were kindly provided by Stem Cell Bank, Chinese Academy of Sciences. For AAV packaging, 10μg of pAAV-RC2 serotype packaging plasmid, 10μg of pAAV-helper plasmid, and 8μg of AAV2 plasmid carrying the construct of interest were transfected to 293T

cells in serum-free DMEM in a 100 mm plate using Lipo6000™ Transfection Reagent (Beyotime, Nanjing, China). The old medium with DMEM-FBS (5% FBS) medium was replaced at the second day. Cells were harvested at 72h post transfection by scraping and pelleting by centrifugation. AAV particles were then purified from the cell pellet according to a previously protocol (Grieger et al., 2006). AAV particles were titred by real-time PCR and adjust to 1×10^{11}v.g/mL (viral genomes/mL) by sterile phosphate buffered saline (PBS)(Veldwijk et al., 2002). Mice were treated with AAV subcutaneous injection at the site of the fourth mammary nipple at the dosage of 10 μL at the age of postnatal day 10 (P10), and made a repeat injection at P12. For comparison, the other side of fourth mammary of each individual mouse was injected with control AAV.

Reagents. Cysteine sulfinic acid (CSA), taurine, and cysteine-Cl were purchased from Sigma-Aldrich chemical company (Sigma, St. Louis, MO, USA). Antibody of CDO, CSAD, and α-SMA were purchased from Abcam (Cambridge, MA, USA). Ki67 antibody was purchased from Cell signaling technology (CST, USA). Antibodies of E-Cadh, K14, K18, K8, PCNA were purchase from ProteinTech Group (Wuhan, China). TUNEL (Terminal-Dexynucleotidyl Transferase (TdT) -Mediated dUTP Nick End Labeling) apoptosis detection kit (FITC) was purchased from YEASEN Biotechnology Co., Ltd (Shanghai, China). All other chemicals were purchased from Sinopharm Chemical Reagent Co., Ltd (Beijing, China).

Animal treatment

Experiments were performed 3 weeks after the following procedure. The WT mice were treated with 200mg/kg body weight (BW) per day cysteine by intraperitoneal injection (i.p.) of cysteine-Cl solution from P21 to P41. CDO KO mice were treated with CSA or taurine, with a dose of 100mg/kg BW per day (Q.D.) from day P21 to P41. After treatment, the mice were anesthetized then their blood was collected and stored at 4˚C for 2 hours for serum collection and sacrificed by cervical fracture. The fourth mammary gland was immediately stripped and frozen in liquid nitrogen for RNA and protein exaction or fixed for histological analysis.

Mammary gland Whole-mount analyses. Fourth inguinal mammary glands were spread onto a cation adsorption microscope slide and fixed overnight in Carnoy's Fluid (Ethanol: chloroform: glacial acetic acid =6:3:1 (v/v/v)) at room temperature (RT). Tissues were rehydrated by incubating in 90% ethanol, 70% ethanol and distilled water, and stained in acetocarmine solution [0.5% (w/v) carmine

(sigma) and 45% (v/v) acetic acid], for 2 hours at RT. Tissues were then dehydrated and by incubating in ethanol gradients (70%, 85%, 95%, and 100% (v/v)) successively and hyalinized by incubation in xylene at RT. Finally, mammary glands were mounted using neutral gum and bright-field images were obtained at 5 fold magnification using the Olympus SZX10 stereo microscope with cellSens Standard 1.9 software. The ductal elongation were measured and the number of branches and TEBs were counted as the average from each whole mount. Data were analyzed by a Student's t test. All values are expressed as means ± SD.

Revers Transcription polymerase chain reaction (RT- PCR) assay. Total RNA was extracted with GeneMark™ Total RNA Purification Kit (GM biolab) according to the manufacturer's instruction. 1 μg of total RNA was reversed transcribed to cDNA with the M-MLV reverse transcriptase (Promega). The primers used for RT-PCR assay were designed using primer-blast (http://www.ncbi.nlm.nih.gov/tools/primer-blast/) and spanning at least one intron. The oligos were purchased from Genewiz Corporation (Suzhou, China) as shown in Table 1.

Western blot assay. The total protein from samples was extracted by homogenization in RIPA lysate and centrifugation. Protein concentrations were determined by a BCA Protein Assay Kit (Beyotime, Nanjing, China), and 50 μg each total protein was loaded and separated in 12% SDS-PAGE and transferred to a PVDF membrane (Millipore). The PVDF membranes were blocked by 5% (wt/vol) non-fat milk diluted in Tween/Tris-buffered saline (TBST), then incubated with primary antibodies (rabbit anti-CSAD (Abcam), rabbit anti-CDO (Abcam), mouse anti-GAPDH (ProteinTech), mouse anti-K14 (ProteinTech), rabbit anti-K18 (ProteinTech), rabbit anti-K8 (ProteinTech), rabbit anti-E-Cadh (ProteinTech), rabbit anti-α-SMA (Abcam), mouse anti-β-Casein (SantaCruz), mouse anti-β-Actin (ProteinTech) diluted in TBST buffer (1:2000~5000) overnight at 4˚C. After washing with TBST, the membranes were incubated with horseradish peroxidase-conjugated secondary antibody (goat anti-rabbit IgG or Goat anti-mouse IgG) (ProteinTech) diluted in TBS (1:20000) for 2 hours at RT. The signals were obtained by exposure X-ray film using chemiluminescence reagent (Milipore), respectively.

Immunohistochemistry (IHC) and immunofluorescence (IF). The mammary gland samples were spread onto a slide, fixed with 4% PFA overnight at 4℃, then embedded in paraffin and sliced into 5 μm sections. After dewaxing and rehydration, antigen retrieval was performed in Tris-EDTA buffer (10 mM Tris, 1 mM EDTA, pH 9.0) by heating and high pressure treatment of the sections.

After being washed with PBS (pH 7.4) for 15 min, non-specific endogenous peroxidase activity was blocked by 3% (vol/vol) H_2O_2 diluted in PBS. Non-specific binding sites were then blocked by 10% normal goat serum diluted in PBS at least for 2 hours at RT. For CDO, K14, K18, K8, E-Cadh, α-SMA and Ki67 detection, the sections were first incubated with each primary antibody (1:100) diluted in PBS overnight at 4˚C. After being washed with PBS for 15 min, the sections were incubated with FITC coupled goat anti-rabbit IgG (1:100) (KPL, San Francisco, CA, USA), FITC coupled goat anti-mouse IgG (1:100) (KPL, San Francisco, CA, USA), Rodmin coupled goat anti-rabbit IgG (1:100) (KPL, San Francisco, CA, USA), or HRP coupled Goat anti-rabbit IgG (1:200) (ProteinTech) for 2 hours at RT. After being washed with PBS for 10 min, finally, the signals were visualized by incubating the sections with 0.05 mol/L Tris-HCL (pH 6.5) containing 0.06% (wt/vol) diaminobenzidine (DAB) and 0.03% (vol/vol) H2O2 or by fluorescence microscope with DP73 camera (Olympus).

Measurement of Taurine. The serum samples were deproteinized by adding methanol to 80% (vol/vol), and centrifuging at 12000 rpm for 20 min, the supernatant was transferred into a clean EP tube for assay. Taurine measurement were followed as previously described (Ma et al., 2015).

Measurement of cysteine sulfinic acid (CSA). The serum samples were deproteinized. The mammary tissue were weighted, homogenized and deproteinized. Protein deposits and tissue fragments were removed by centrifugation. The supernatant of serum samples and mammary samples were purified by flowing through a strong cation exchanger resin (SCX) (Solarbio, Beijing China) column and the effluent was then loaded it onto a strong anion exchanger resin (SAX) (Solarbio, Beijing China) column for solid phase extraction (SPE). CSA was attached to SAX and subsequently eluted using 30% (v/v) formic acid and spinning. A certain concentration of L-glutamine (200 μM) was added to the samples as an internal standard. The samples were mixed with an o-Phthalaldehyde (OPA) solution for CSA derivatization and filtrated using a 0.22 μm filter (Millipore) before loading. The mobile phase of HPLC was 1% formic acid and 45% methanol. The HPLC method was the same as taurine measurement. Because CSA could be further oxidized to cysteic acid (CA) after exposure to oxygen, the total CSA in tissue should be composed of CA and CSA (Eleni et al., 2010). The retention time for glutamine, CA, and CSA was around 19.4 min, 4.7 min, and 8.7 min, respectively.